

**Synthesis, Characterization and Photocatalytic property of  
halide double perovskites  $Cs_2Ag_{(1-x)}Na_xInCl_6$**

A Dissertation for  
**PHY651: Dissertation**  
**Credits: 16**  
Submitted in partial fulfillment of Masters Degree

**M.Sc in Physics**  
Goa University  
In the subject of Physics

by

**Cedric Pires**  
22P0430006  
ABC ID:335694068973  
PRN:20190236

Under the supervision of  
**Dr.Venkatesha R Hathwar**

School Of Physical and Applied Sciences  
Physics discipline



**Goa University**  
May 2024



Seal of the School

Examined by:

## **DECLARATION BY STUDENT**

I hereby declare that the data presented in this Dissertation report entitled, **Synthesis, Characterization and Photocatalytic property of halide double perovskites  $Cs_2Ag_{(1-x)}Na_xInCl_6$** , is based on the results of investigations carried out by me in the **School of Physical and Applied Sciences** at the **Goa University** under the Supervision of **Dr. Venkatesha .R. Hathwar**. I further declare that the same has not been submitted elsewhere for the award of a degree or diploma by me.

Further, I understand that Goa University or its authorities will not be responsible for the correctness of observations / experimental or other findings given in the dissertation.

I hereby authorize the University authorities to upload this dissertation on the dissertation repository or anywhere else as the UGC regulations demand and make it available to anyone as needed.

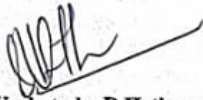
Date: May 6, 2024  
Place: Goa University



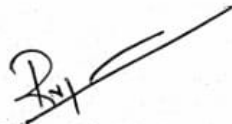
**Cedric Nibel Pires**  
**22P0430006**

## COMPLETION CERTIFICATE

This is to certify that the dissertation report "**Synthesis, Characterization and Photocatalytic property of halide double perovskites  $CS_2Ag_{(1-x)}Na_xInCl_6$** " is a bonafide work carried out by Mr Cedric Nibel Pires under my supervision in partial fulfilment of the requirements for the award of the degree of Masters of Science in Physics in the Discipline Physics at the **School of Physical and Applied Sciences** at the **Goa University**.



**Dr. Venkatesha R Hathwar**  
Date: May 6, 2024



Signature of Dean of the School  
Date: May 6, 2024  
Place: Goa University



Dept stamp

## ACKNOWLEDGEMENT

This thesis would not have been possible without the guidance and the help of several individuals, who in one way or another contributed and extended their valuable assistance in the preparation and completion of this study, it is a pleasure to thank those who made it a possibility.

I am grateful to Dr. Venkatesha Hathwar for entrusting me with the opportunity to undertake this project. His guidance and expertise proved invaluable in navigating the complexities of my topic. I am deeply grateful for his unwavering commitment to my academic development.

I would particularly like to thank to Mr. Irshad Shaikh for his constant guidance and expertise in the topic that strengthened my methodology and analysis. His unwavering support throughout the research was invaluable.

My thanks to Mr Mahendra Choudhary for his help in navigating through various instruments and equipment which contributed greatly to the progression of the project.

I would like to thank the School of Physical and Applied Sciences for providing the necessary instruments and infrastructure that underpinned my research efforts.

I am thankful to the faculty of Physics, whose insightful teaching throughout my M.Sc. program provided the critical knowledge and analytical skills crucial for undertaking this research.

Finally, I would also like to extend my sincere thanks to my family and friends for their unwavering support and encouragement during this challenging journey.

# Contents

<b>1</b>	<b>Introduction</b>	<b>9</b>
1.1	Dyes . . . . .	9
1.2	Toxicity of Dyes . . . . .	11
1.3	Techniques for dye detection . . . . .	12
1.4	Prevention . . . . .	13
1.5	Perovskites . . . . .	15
1.5.1	Hallide Perovskites . . . . .	17
1.5.2	Advantages of Perovskites for Dye Degradation: . . . . .	17
1.5.3	Lead hallide Perovskite . . . . .	17
1.6	Lead Free Hallide Perovskite . . . . .	18
1.7	$Cs_2AgInCl_6$ . . . . .	19
1.8	Literature Review . . . . .	21
1.9	Aims and Objectives . . . . .	22
<b>2</b>	<b>Synthesis</b>	<b>23</b>
2.1	Materials . . . . .	23
2.2	Synthesis Process . . . . .	24
2.2.1	Procedure . . . . .	24
<b>3</b>	<b>Characterization</b>	<b>26</b>
3.1	X-Ray Diffraction (XRD) . . . . .	26
3.1.1	Principle of XRD . . . . .	26
3.1.2	Working of XRD . . . . .	26
3.1.3	Advantages and Disadvantages of XRD . . . . .	26
3.1.4	Single Crystal XRD vs Powder XRD . . . . .	27
3.1.5	Interaction of X-rays with matter . . . . .	27
3.1.6	Powder XRD . . . . .	28
3.1.7	Powder XRD method . . . . .	28
3.1.8	Powder X-ray Diffractometer . . . . .	29
3.1.9	Applications . . . . .	29
3.1.10	Advantages and disadvantages of X-ray Powder Diffraction (XRD) . . . . .	29
3.2	Ultraviolet-visible (UV-Vis) spectroscopy . . . . .	31
3.2.1	The principle of UV . . . . .	31
3.2.2	Beer-Lambert Law . . . . .	32
3.2.3	Instrumentation . . . . .	33
3.2.4	Working . . . . .	34
3.3	Scanning Electron Microscopy (SEM) . . . . .	37
3.3.1	Principle of SEM . . . . .	37
3.3.2	Instrumentation . . . . .	38
3.3.3	Advantages and disadvantages of SEM . . . . .	38
3.3.4	Applications . . . . .	39
3.4	Photocatalysis . . . . .	41
3.4.1	Mechanism . . . . .	42
3.4.2	Photocatalytic Mechanism of $Cs_2Ag_{(1-x)}Na_xInCl_6$ . . . . .	44
3.4.3	Factors affecting photocatalysis . . . . .	45
<b>4</b>	<b>Results and Discussion</b>	<b>46</b>
4.1	X Ray Diffraction (XRD) . . . . .	46
4.2	Scanning Electron Microscopy (SEM) . . . . .	49
4.3	Photocatalysis . . . . .	50
4.3.1	Comparison with other published works . . . . .	52
<b>5</b>	<b>Conclusion</b>	<b>53</b>

## List of Figures

1	Examples of Azo dyes.[4] . . . . .	10
2	Anthroquinone Dyes example[7] . . . . .	10
3	Examples of Phtalocayne dyes. [29] . . . . .	11
4	Exmples of Nitro/ Nitroso dye [31] . . . . .	11
5	Diagram of the structure of Perovskites . . . . .	15
6	Diagram of the structure of hallide Perovskite . . . . .	15
7	Diagram of the structure of Double Hallide Perovskites . . . . .	16
8	Structure of Perovskite $Cs_2AgInCl_6$ [33] . . . . .	19
9	Degradation of organic dyes by (d) $Cs_2AgInCl_6$ and (b) $Cs_2Ag_{(1-x)}Na_xInCl_6$ [38] [64] . . .	21
10	Precursor materials used in synthesis . . . . .	23
11	Schematic diagram of the process of Acid Precipitation synthesis . . . . .	24
12	Figures shown: fig a.stirring process,figs b,c.Sample after drying . . . . .	25
13	Generation of $CuK\alpha$ radiaton and X Ray spectrum of Cu [67] . . . . .	26
14	Bragg's Law reflection. The diffracted X-rays exhibit constructive interference when the distance between paths ABC and A'B'C' differs by an integer number of wavelengths ( $\lambda$ ) [16] . . .	27
15	Formation of the cone of a diffracted beam. Adopted from reference [70] . . . . .	28
16	Rigaku Smart Lab Powder X-ray diffractometer at ULMC of Goa University. . . . .	30
17	Electronic transitions in UV-Visible spectroscopy.[73] . . . . .	31
18	Schematic diagram of UV- visible spectrophotometer.[10] . . . . .	33
19	Simple Schematic diagram of UV- visible spectrophotometer.[1] . . . . .	34
20	Schematic diagram of a cuvette-based UV-Vis spectroscopy system.[14] . . . . .	35
21	Simple Schematic diagram of SEM.[45] . . . . .	37
22	Simple Schematic diagram of SEM.[58] . . . . .	38
23	Carl Zeiss Scanning Electron Microscope at USIC of Goa University. . . . .	40
24	Schematic diagram of mechanism of photocatalysis [19] . . . . .	42
25	Photochemical Reactor at SPAS, Goa University . . . . .	43
26	X ray Diffraction Patterns of synthesized $Cs_2Ag_{(1-x)}Na_xInCl_6$ . . . . .	46
27	Profile matching for the series of $Cs_2Ag_{(1-x)}Na_xInCl_6$ . Where x=0 . . . . .	47
28	Profile matching for the series of $Cs_2Ag_{(1-x)}Na_xInCl_6$ . Where x=0.4 . . . . .	47
29	Profile matching for the series of $Cs_2Ag_{(1-x)}Na_xInCl_6$ . Where x=0.5 . . . . .	48
30	Profile matching for the series of $Cs_2Ag_{(1-x)}Na_xInCl_6$ . Where x=0.6 . . . . .	48
31	SEM image of series $Cs_2Ag_{(1-x)}Na_xInCl_6$ with scale in all fig equal to $2\mu m$ . . . . .	49
32	UV-Vis absorption spectra for Methyl Orange degradation in the presence of the series of $Cs_2Ag_{(1-x)}Na_xInCl_6$ double perovskites under various UV-light irradiation times (The inset shows the change of solution colour) . . . . .	50
33	Plots of $C_t/C_0$ versus the irradiation time for photocatalytic degradation of Methyl Orange in the presence of $Cs_2Ag_{(1-x)}Na_xInCl_6$ . . . . .	51
34	Kinetic Curves of photocatalytic degradation reaction of Methyl Orange . . . . .	51
35	Degradation of organic dyes by (d) $Cs_2AgInCl_6$ and (b) $Cs_2Ag_{(1-x)}Na_xInCl_6$ [38] [64] . . .	52

## List of Tables

1	Compound, Lattice Parameter, and Direct Cell Volume . . . . .	46
2	Compound and Time (min) . . . . .	50
3	Dye Degradation Constant (k value) . . . . .	51

## ABSTRACT

This study investigates the photocatalytic degradation of the organic dye pollutant, Methyl Orange (MO), using Na-doped  $Cs_2AgInCl_6$  double halide perovskites. Perovskite materials were synthesized with varying Na concentration ( $x = 0, 0.4, 0.5, 0.6$ ) via the acid precipitation method. X-ray diffraction (XRD) and scanning electron microscopy (SEM) were employed to characterize the crystal structure and morphology of the synthesized photocatalysts. The photocatalytic activity of the materials was then evaluated by monitoring the degradation of Methyl Orange under simulated sunlight irradiation. Results demonstrate that all Na-doped perovskites exhibit photocatalytic activity towards MO degradation. Notably, the compound with  $x = 0.5$  displayed the most efficient dye removal, suggesting an optimal Na doping level for enhanced photocatalytic performance. This work highlights the potential of Na-doped  $Cs_2AgInCl_6$  double halide perovskites as promising photocatalysts for organic pollutant degradation.

# 1 Introduction

Color is the world's vibrant language, adorning our creations and captivating our senses since times immemorial. The world we inhabit is a captivatingly colorful canvas, not just a random arrangement of matter. Color, in its infinite variety and intensity, serves as a fundamental language shaping our perception of the physical landscape and the objects we create.

From the vibrant plumage of exotic birds to the delicate blush of a budding rose, color imbues our environment with meaning and aesthetic significance [9]. This ubiquitous presence of color transcends the realm of nature, playing a pivotal role in human culture and industry.

With the onset of industrialization, the use of color has exploded. Driven by the desire to enhance product appeal and attract consumers, industries pursued the expansion of the color spectrum available to them relentlessly. This pursuit has yielded a vast arsenal of synthetic dyes and pigments, capable of conjuring almost any imaginable shade or hue [26]. This explosion of color has completely altered the visual landscape of our world, transforming manufactured goods into vibrant representations of human ingenuity and desire.

Beyond all the enhancing of brand identity and influencing consumer behavior, color in industrial products casts a dark shadow on the environment. Organic dye waste from industrial processes pollutes water bodies, leading to aesthetic degradation and impeding of recreational activities. These dyes are, more often than not, toxic to aquatic life, disrupting the food chain through bioaccumulation and direct mortality [61].

## 1.1 Dyes

Industries employing toxic organic dyes, such as paint, varnish, textiles, plastics, ink, and cosmetics, raise pressing environmental concerns. These dyes' complex structures hamper wastewater treatment, leading to persistent contamination of water and soil [28].

Their prolonged presence poses concerning ecological risks and necessitates immediate action. Shifting towards environmentally sustainable alternatives and adopting responsible production practices to minimize harmful pollution are crucial steps industries must take to ensure environmental and public health are prioritized.

Dyes are substances capable of imparting color by chemically or physically binding with materials. Unlike most organic compounds, dyes possess colour because they

1. absorb light in the visible spectrum (400–700 nm),
2. have at least one chromophore (colour-bearing group),
3. have a conjugated system, i.e. a structure with alternating double and single bonds, and
4. exhibit resonance of electrons, which is a stabilizing force in organic compounds [62]

While the quality of dyes varies with the manufacturer, the dyes which take less time to colour the fabric and are chemically stable are most preferable. Dyeing the fabric forms strong chemical bonds between dye molecules and the fabric. Temperature and time are two important factors that determine the durability of the dye.

There are various types of organic dyes that are commonly used in industries for coloring and printing purposes. Some of the most common types of organic dyes include:

- Azo dyes:

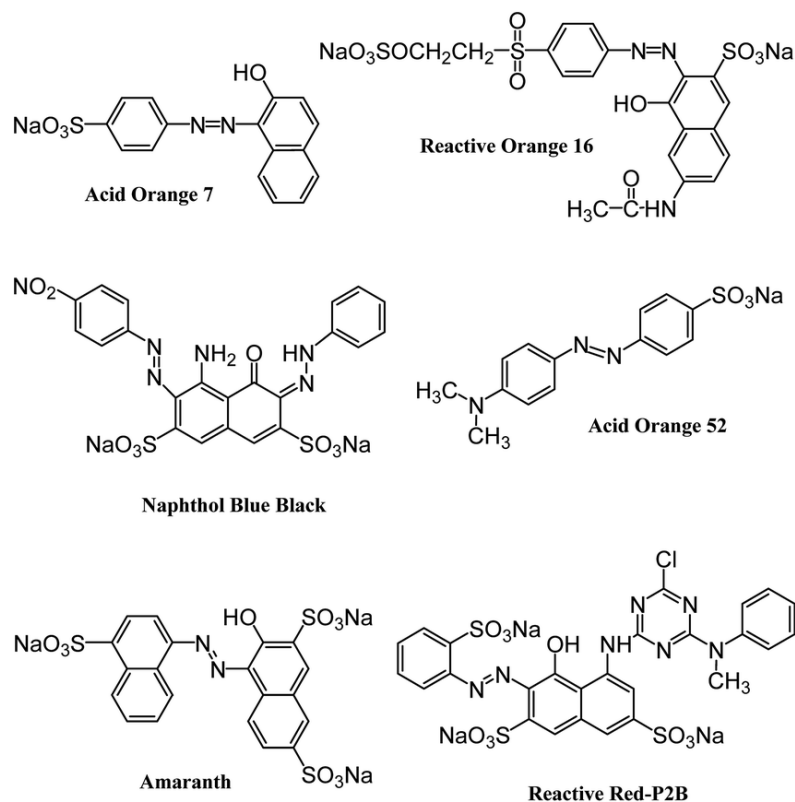


Figure 1: Examples of Azo dyes.[4]

These dyes are derived from the azo group ( $-\text{N}=\text{N}-$ ) and can have a range of colors. These are the most widely used organic dyes and are commonly used in the textile and leather industries. Some samples of popular azo dyes are- methyl orange azo dye- widely used in textiles, dimethylamino azobenzene- which is the name of the red azo dye, benzene azo beta naphthol, etc.

- Anthraquinone dyes:

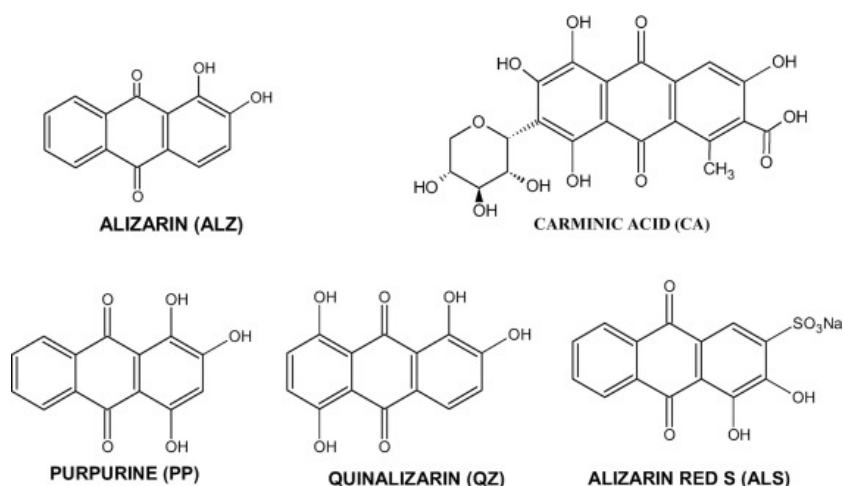


Figure 2: Anthraquinone Dyes example[7]

These dyes are derived from anthraquinone, a compound found in plants. They are commonly used in the production of textiles, plastics, and printing inks.

- Phthalocyanine dyes:

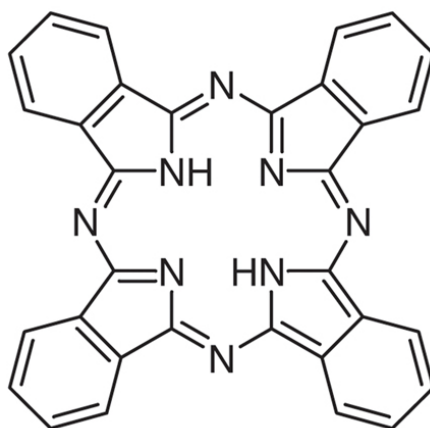


Figure 3: Examples of Phthalocyanine dyes. [29]

These dyes are used in the production of inks, coatings, and plastics. They are known for their bright blue and green colors and are often used in printing applications.

- Nitro dyes:

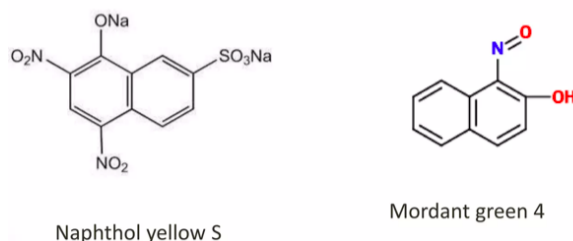


Figure 4: Examples of Nitro/ Nitroso dye [31]

These dyes are used in the production of dyes for cellulose fibers and are known for their bright and vibrant colors.

- Natural dyes: These dyes are derived from natural sources such as plants, insects, and minerals. They are often used in the production of textiles and are considered to be more environmentally friendly than synthetic dyes.

Each type of dye can have different environmental impacts if not properly managed and treated before discharge into water bodies.

## 1.2 Toxicity of Dyes

These pigments that adorn our clothes, textiles, and even food, hold a potential for toxicity that can impact human health and the environment. While their aesthetic appeal is undeniable, the chemical composition and processing of certain dyes pose significant risks [42].

Organic dyes, known for their chemical complexity, pose a significant threat to aquatic life. Their structure, often laced with aromatic compounds or other harmful groups, can inflict cellular damage and disrupt vital physiological processes [65]. Azo dyes for instance, their breakdown releases carcinogenic aromatic amines, poisoning fish and infiltrating the food chain with its toxic tendrils [52]. Studies have linked exposure to these amines to an increased risk of bladder cancer in dye industry workers [52]. Additionally, the wastewater generated during dye production can contain toxic chemicals that contaminate water sources and harm aquatic ecosystems [52].

Dyes act as light thieves, impeding photosynthesis and disrupting the delicate balance of aquatic ecosystems. Their ability to chelate metal ions further worsens the problem, inducing micro-toxicity in fish and other vul-

nerable organisms [65]. The relentless cycle of oxidation and reduction that dyes undergo in water releases toxic intermediates, further jeopardizing the health of aquatic life [65].

The toxic nature of these dyes are a threat to human health as well. Studies have linked exposure to certain organic dyes, particularly those with carcinogenic properties, to an increased risk of cancer in humans [3]. Their ability to interact with DNA and induce mutations can trigger the uncontrolled growth of cells, potentially leading to the development of tumors [52].

Textile dyes can migrate from clothing onto skin, potentially causing allergic reactions and dermatitis [28]. Furthermore, the use of certain dyes in food can have negative consequences. Some studies suggest that synthetic food dyes might contribute to hyperactivity and behavioral problems in children [17].

The remnants of these dyes also pose a challenge during water purification processes as their combination of complex structures often resist degradation, leaving behind a lingering presence that continues to disrupt the balance of aquatic ecosystems [52].

### 1.3 Techniques for dye detection

Dyes can be detected using a variety of techniques

#### 1. Spectroscopic Techniques:

##### (a) Ultraviolet-Visible (UV-Vis) Spectroscopy:

This technique involves measuring the absorption or transmission of ultraviolet and visible light by the dye molecule. Organic dyes tend to absorb light in the visible range, which can be used for identifying and quantifying individual dyes [66] [14]

(Image of Ultraviolet-Visible (UV-Vis) Spectrometer)

##### (b) Fluorescence Spectroscopy:

Organic dyes can often emit fluorescent light when excited by a specific wavelength of light. Fluorescence spectroscopy measures this emission, which can be used to identify and quantify the dye [35].

#### 2. Chromatographic Techniques:

##### (a) High-Performance Liquid Chromatography (HPLC):

HPLC is a chromatographic technique that separates compounds based on their solubility and interaction with a stationary phase. Organic dyes can be separated and detected using HPLC, which can provide information about their identity and concentration [41].

Different HPLC variants, like UV-Vis HPLC and LC-MS/MS, provide valuable information about the dyes' spectral properties and molecular identities. (Image of High-Performance Liquid Chromatography (HPLC) setup)

##### (b) Thin-Layer Chromatography (TLC):

This simple yet effective technique offers a quick visual screening of dye samples. Separated components appear as distinct spots on a plate due to their differential migration along the stationary phase. TLC is ideal for preliminary identification and purity checks. (Image of Thin-Layer Chromatography (TLC) plate)

#### 3. Spectroscopic Techniques:

##### (a) Ultraviolet-Visible (UV-Vis) Spectroscopy: This technique shines a light on the dyes' inherent colors. By measuring the absorption of light at different wavelengths, UV-Vis spectroscopy can provide characteristic fingerprints for identifying specific dyes.

This technique involves measuring the absorption or transmission of ultraviolet and visible light by the dye molecule. Organic dyes tend to absorb light in the visible range, which can be used to identify and quantify the dye [14].

##### (b) Fluorescence Spectroscopy: Some dyes possess the ability to emit light at a different wavelength upon excitation. Organic dyes can often emit fluorescent light when excited by a specific wavelength of light. Fluorescence spectroscopy measures this emission, which can be used to identify and quantify the dye.

#### 4. Mass Spectrometry (MS):

This powerhouse technique provides definitive molecular fingerprints of dyes. By ionizing and fragmenting the dye molecules, MS reveals their mass-to-charge ratios, enabling identification and even structural elucidation. Coupling MS with chromatographic techniques like LC-MS/MS further enhances sensitivity and specificity [46].

#### 5. Other Techniques:

**Infrared Spectroscopy:** Infrared spectroscopy involves measuring the absorption of infrared light by a molecule. Organic dyes have unique infrared spectra that can be used to identify and quantify them.

- (a) **Fourier-Transform Infrared (FTIR) Spectroscopy:** This technique probes the vibrational modes of dye molecules, providing information about their functional groups and chemical composition. It can be particularly useful for differentiating between structurally similar dyes.
- (b) **Raman Spectroscopy:** This technique analyzes the inelastic scattering of light by molecules, offering complementary information about the vibrational modes and structural details of dyes. It can be particularly effective for analyzing dyes in complex matrices where other techniques might struggle.

While the above mentioned techniques can be used to detect some dyes, Detection of specific dyes or multiple in effluents is a challenge, because, even though dyes are highly colored molecules, their spectrophotometric detection is not possible due to interference of spectral lines in a mixture containing a number of dyes including, R6G, RhB, MB, , methyl orange (MO), methyl red (MR), acridine orange (AO), indigo carmine (IC), methyl violet (MV), etc.

Therefore, the direct determination of these dyes in wastewater effluents is strenuous and cost- intensive and thus requires special techniques and procedures.

## 1.4 Prevention

While organic dyes undoubtedly play a significant role in diverse industries, their potential toxicity towards human health and the environment, necessitates an urgent call for action. Fortunately there exist, several key strategies that offer promising avenues for minimizing the negative impacts associated dyes. Some of these include:

#### 1. Embracing Sustainable Dye Choices:

**Shifting Towards Bio-Based Dyes:** Exploring and adopting natural dyes derived from plants, bacteria, and other renewable sources presents an eco-friendly alternative. These dyes often exhibit lower toxicity and biodegradability compared to synthetic counterparts [65].

#### 2. Utilizing Dyes Derived from Byproducts:

Exploring innovative methods to utilize byproducts from industries like food processing as sources for dyes not only promotes resource efficiency but also reduces the reliance on synthetic dye production [28].

#### 3. Implementing Responsible Production and Usage Practices:

**Enforcing Stricter Regulations:** Establishing and enforcing stringent regulations on dye production, including limitations on the use of hazardous chemicals and stricter wastewater treatment standards, can be crucial for minimizing environmental pollution [13].

**Utilizing Closed-Loop Production Systems:** Integrating closed-loop systems within dye manufacturing facilities aims to minimize water usage and maximize water and dye recycling, significantly reducing wastewater discharge and the concerns associated with it [65].

**Promoting Cleaner Production Technologies:** Encouraging the adoption of cleaner production technologies in dye industries, such as supercritical fluid dyeing and enzymatic dyeing, can reduce water and energy consumption while minimizing chemical waste [65].

#### 4. Optimizing Wastewater Treatment Strategies:

**Advanced Oxidation Processes:** Implementing advanced oxidation processes like ozonation and photocatalysis can effectively degrade recalcitrant organic dyes present in wastewater effluents, mitigating their negative environmental impact [65].

Adsorption Techniques: Utilizing low-cost adsorbents such as activated carbon or biochar can be an effective strategy for removing dye pollutants from wastewater effluents [63].

Development of Biosorbents: Exploring the potential of microbial biomass or agricultural residues as biosorbents offers a sustainable and cost-effective solution for dye removal from wastewater[65].

5. Enhancing Consumer Awareness and Responsibility:

Supporting Eco-Friendly Textile Brands: Consumers play a crucial role by opting for clothing and products dyed using more sustainable practices and advocating for environmentally conscious brands [13].

Implementing Proper Disposal Methods: Encouraging proper disposal practices for dyed textiles to avoid contamination of landfills and wastewater systems is essential [32].

Overall, preventing the negative impact of organic dyes on water bodies requires a combination of proper waste management practices, the use of eco-friendly dyes, and a sustainable manufacturing process. By implementing these measures, companies can minimize their impact on the environment and protect water bodies from harmful pollutants. In addition, regulatory agencies may impose restrictions on the use of certain organic dyes in order to protect human health and the environment.

## 1.5 Perovskites

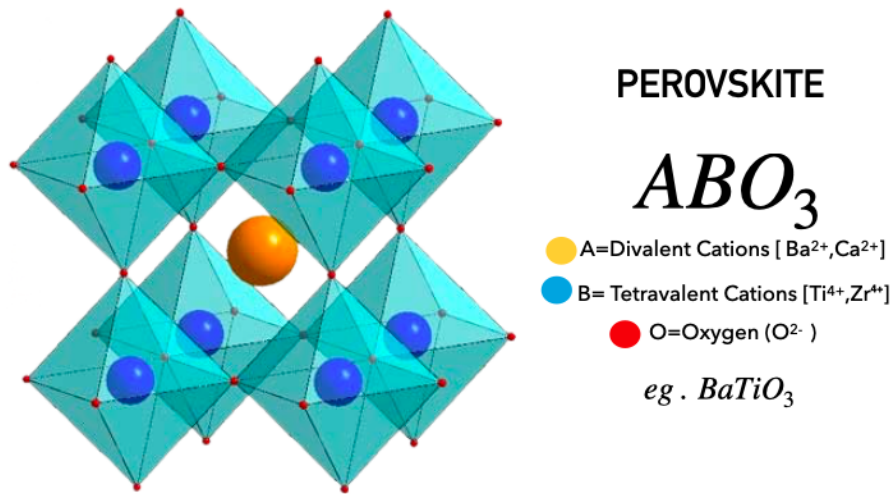


Figure 5: Diagram of the structure of Perovskites

Perovskites, due to their versatile structure and novel optoelectronic properties, have seen a rise as promising candidates for applications on photocatalysis, which includes the photodegradation of organic dyes [23]. Perovskites possess a general formula of [20]



Where

- A is a divalent cation ( $Ba^{2+}, Ca^{2+}$ ),
- B is a tetravalent cation ( $Ti^{4+}, Zr^{4+}$ ), and
- X is an anion (O).

Hallide perovskites possess the general formula

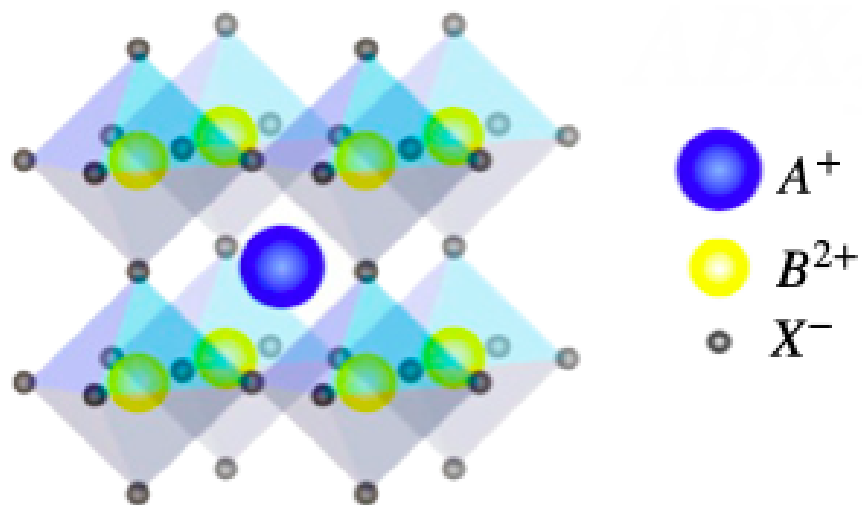


Figure 6: Diagram of the structure of halide Perovskite



Where:

- A is a monovalent cation ( $Cs^+$ ,  $CH_3NH_3^+$ ),
- B is a divalent cation ( $Pb^{2+}$ ,  $Sr^{2+}$ ), and
- X is an anion ( $Cl^-$ ,  $Br^-$ ,  $I^-$ ).

Within this family, double perovskites (DPs) represent a specific subgroup with a distinct crystal structure and intriguing properties compared to their single perovskite counterparts[43].

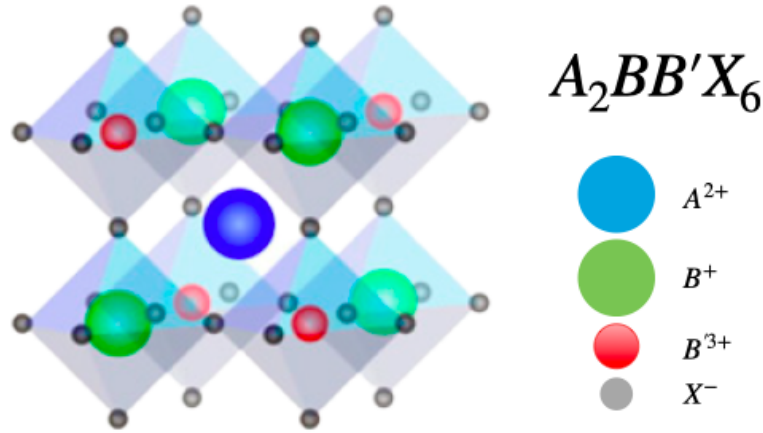


Figure 7: Diagram of the structure of Double Hallide Perovskites

Double Perovskites have the general formula of



where,

- $A = A^{2+}$  divalent cation
- $B = B^+$  monovalent cation
- $B = B^{3+}$  trivalent cation
- $O = O^-$  oxygen

The change in structure brings about more properties that find more applications, often enhancing what the single Perovskite structure would offer [34]. Structurally,

- Single Perovskites: In a single perovskite, the A cation typically occupies a large cavity at the center of the unit cell, while the B cation and X anion form a corner-sharing  $BX_6$  octahedral network [20]. This arrangement allows for a high degree of tolerance for different cation sizes due to the flexibility of the A-site.
- Double Perovskites: Double perovskites possess a more complex structure with the general formula  $A_2BB'X_6$ . Here, the A cations occupy the same large cavities as in single perovskites. However, the crucial difference lies in the B-site, which is occupied by two distinct cations, B and B' [60]. These B cations order themselves in a specific way, typically adopting a rock-salt-like arrangement, leading to corner-sharing  $BO_6$  and  $B'X_6$  octahedra[25].

The presence of two distinct B-cations in DPs offers several advantages and introduces some key differences compared to single perovskites:

- Tailoring Functionality: The controlled introduction of different B-cations allows for a wider range of property tuning in DPs. This can be exploited to achieve specific magnetic, electronic, or optical functionalities[47].
- Enhanced Stability: The ordered B-site cation arrangement in DPs can lead to improved structural stability compared to some single perovskites, particularly when dealing with cations with a large size difference [30].

This results in a flexible structure that allows for cation and anion substitutions, enabling bandgap engineering and tailoring of properties for specific applications.

### 1.5.1 Hallide Perovskites

Halide perovskites have been receiving a lot of attention in recent years due to their excellent optoelectronic properties.

They have a perovskite crystal structure which is usually composed of a metal halide framework (such as lead, tin, or cesium) and an organic cation (such as methylammonium or formamidinium) such as methylammonium lead iodide ( $MAPbI_3$ ) or formamidinium lead iodide ( $FAPbI_3$ ) which are widely studied.

### 1.5.2 Advantages of Perovskites for Dye Degradation:

Perovskite photocatalysts offer several advantages compared to traditional photocatalysts like  $TiO_2$ , these include

1. Tunable Bandgap: Bandgap engineering through cation/anion substitution makes way for tailoring the light absorption properties of the photocatalyst to target specific dyes and achieve efficient degradation under variable light sources and light availability.
2. High Absorption Coefficient: Many perovskites exhibit strong light absorption across a broad spectrum, leading to efficient utilization of light for photocatalysis.
3. Long Charge Carrier Lifetime: Extended lifetimes of charge carriers in certain perovskites allow for more efficient utilization of generated charges before recombination thereby, enhancing photocatalytic activity.

### 1.5.3 Lead hallide Perovskite

Lead-based perovskites (LHPs) have emerged as promising candidates as materials for environmental remediation, particularly in the degradation of organic pollutants within wastewater [47]. They possess the general formula:



where,

- A is a monovalent cation
- B is a divalent cation, which in this case, is lead ( $Pb^{2+}$ )
- X is an anion

LHPs exhibit a unique crystal structure with excellent optoelectronic properties. These properties, which include tunable bandgaps, strong light absorption etc make LHPs ideal for applications in solar cells and other sustainable energy related fields [71] which has attracted immense attention towards them. There has been research that has delved into the potential of LHPs for environmental remediation, specifically, the degradation of organic pollutants in water. Through the process of photocatalysis.

Through all this research we know that, LHPs have demonstrated remarkable efficacy in removing diverse pollutants, including dyes, pesticides, and pharmaceuticals [22][72] by the process of photocatalysis. The mechanism of photocatalysis involves absorption of light by the perovskite, leading to the generation of reactive oxygen species (ROS) that degrade and break down the target pollutants [22].

However, despite their promising performance, LHPs have a significant downside – their lead content. Lead is a well-documented toxic heavy metal, posing severe health risks to humans and wildlife through ingestion, inhalation, or skin contact [37]. The potential for lead leaching from LHPs during synthesis, usage, or disposal raises immense environmental and safety concerns, hindering their widespread application [37].

Additionally, LHPs often exhibit poor stability under light and moisture exposure, leading to decomposition and further exacerbating the lead release issue [55]. Lead toxicity has a range of negative effects on the body, including damage to the nervous system, kidneys, and reproductive system. Children and pregnant women are particularly vulnerable to the harmful effects of lead, which can lead to developmental delays and neurological problems.

Therefore, While lead-based perovskites have shown great promise for degrading organic pollutants in water, the potential risks associated with lead exposure must be considered carefully. To reduce the potential risks of lead toxicity, it is vital to implement safe handling and disposal practices for materials containing any amount of lead.

This also includes following proper safety protocols when working with lead based perovskites or other lead-containing materials, such as wearing protective equipment and proper disposal of waste materials. Exploring alternative materials that do not contain lead, such as lead-free perovskites, is also a very viable option, so as to minimize the potential risks associated with lead toxicity.

## 1.6 Lead Free Hallide Perovskite

Lead free hallide Perovskites have attracted considerable attention in recent years, particularly when it comes to photocatalysis of organic pollutants. These materials, free from the inherent toxicity concerns associated with lead-based counterparts, have emerged as promising candidates for environmental remediation and energy applications, aligning with sustainable development goals [55]. More than just environmental consciousness, they inherit advantageous properties from their lead-containing brethren:

1. **Exceptional Light Absorption:** Lead-free perovskites exhibit remarkable light absorption across a broad spectrum. This capability stems from their high charge carrier mobility and extended carrier lifetimes, leading to efficient capture and transport of generated carriers [71].
2. **Tunable Band Gap:** By manipulating the composition and crystal structure of lead free hallide Perovskites, the band gap of these materials can be tailored, enabling them to effectively absorb light across a wider range of the solar spectrum. This property holds great potential for optimizing performance in applications like solar cells [48].

These desirable properties translate into promising avenues associated to the process of photocatalysis:

- **Water Splitting:** By harnessing the power of sunlight, lead-free perovskites show potential for splitting water into hydrogen and oxygen, offering a clean and sustainable avenue for fuel production [5].
- **Organic Pollutant Degradation:** These materials demonstrate remarkable effectiveness in breaking down harmful pollutants like dyes and pharmaceuticals, which is often challenging to remove using conventional methods [72][22][19].

Additionally, their tunable band gaps allow for strategic targeting of specific pollutants by manipulating light absorption.

Intense research efforts are exploring diverse compositions to unlock the full potential of lead-free perovskites:

$Cs_2AgInCl_6$  and  $Cs_2AgBiBr_6$ , belonging to the class of double perovskites, showcase remarkable photocatalytic activity in pollutant degradation, highlighting their promising future [72][33].

Compositions containing elements like tin, germanium, and antimony are actively being investigated to further optimize performance and stability [55]. However, even with these materials showing captivating possibilities, certain challenges still remain, these are:

- **Long-Term Stability:** Ensuring consistent and reliable performance over extended periods under operational conditions demands further investigation [71].
- **Efficiency Optimization:** Although advancements are being made, there's still plenty of room for improvement in photocatalytic efficiency to compete with established technologies.

Despite these challenges, the progress made on lead-free perovskites offers a hopeful outlook for photocatalysis and the other applications related to it. With continued efforts to overcome limitations and explore novel compositions, these environmentally friendly materials hold immense promise for sustainable water purification, pollutant degradation, and other applications.

### 1.7 $Cs_2AgInCl_6$

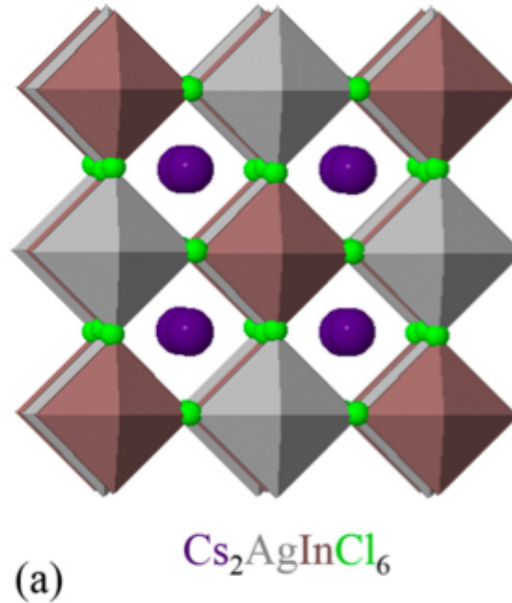


Figure 8: Structure of Perovskite  $Cs_2AgInCl_6$  [33]

Among the burgeoning field of lead-free halide perovskites,  $Cs_2AgInCl_6$  has emerged as a particularly captivating material, attracting significant attention for its intriguing properties and promising applications. Unlike its lead-based counterparts, which pose environmental and health concerns,  $Cs_2AgInCl_6$  offers a sustainable alternative while showcasing remarkable performance in several areas [33].

#### 1. Crystalline Structure and Composition:

$Cs_2AgInCl_6$  possesses a double perovskite structure, where the A-site is occupied by cesium ( $Cs^+$ ) cations and the B-site is shared by silver ( $Ag^+$ ) and indium ( $In^{3+}$ ) cations. This unique structure, combined with the specific choice of elements, contributes to the material's exceptional properties.

#### 2. Key Properties:

- **Broad Light Absorption:**  $Cs_2AgInCl_6$  exhibits exceptional light absorption across a wide spectrum, encompassing both visible and near-infrared light. This stems from its favorable band structure and low defect density, allowing efficient capture and utilization of light energy [40][2].
- **Tunable Band Gap:** The band gap of  $Cs_2AgInCl_6$  can be tailored to a certain extent by manipulating its composition or incorporating dopants. This enables fine-tuning its light absorption range for specific applications, such as solar cells or photocatalysis [2][40].
- **High Stability:** Compared to many lead-based perovskites,  $Cs_2AgInCl_6$  demonstrates notable stability under ambient conditions. It exhibits lower sensitivity to moisture and light exposure, making it a more attractive option for long-term applications [40].

#### 3. Promising Applications:

- **Photocatalysis:**  $Cs_2AgInCl_6$  has shown remarkable activity in photocatalytic processes, including the degradation of organic pollutants and water splitting. Its efficient light absorption and tunable band gap allow for targeted degradation of pollutants and efficient conversion of sunlight into hydrogen fuel [38][2] [40].

- Photovoltaics: While still under development,  $Cs_2AgInCl_6$  holds potential for photovoltaic applications due to its light absorption properties and tunable band gap. Further research on improving its charge transport and device stability is needed [2] [39].
- Optoelectronics: The tunable band gap and unique optoelectronic properties of  $Cs_2AgInCl_6$  make it a potential candidate for various optoelectronic devices, such as light-emitting diodes (LEDs) and photodetectors [39]. However, further exploration and optimization are necessary [68].

#### 4. Challenges and Future Prospects:

Despite its promising properties,  $Cs_2AgInCl_6$  still faces some challenges [8][44]:

- Long-Term Stability: While exhibiting improved stability compared to lead-based counterparts, further enhancements are needed for robust performance in real-world applications.
- Efficiency Optimization: While demonstrating considerable photocatalytic activity, further improvements in efficiency are crucial for wider adoption in applications like water treatment and fuel production.
- Fabrication Methods: Developing scalable and cost-effective fabrication methods is essential for the practical implementation of  $Cs_2AgInCl_6$  in various technologies.

Despite these challenges, the ongoing research efforts on  $Cs_2AgInCl_6$  offer a promising outlook. With continued advancements in understanding its properties, optimizing its performance, and developing efficient fabrication methods, this lead-free perovskite holds immense potential to contribute to sustainable solutions in photocatalysis, photovoltaics, and other optoelectronic applications.

## 1.8 Literature Review

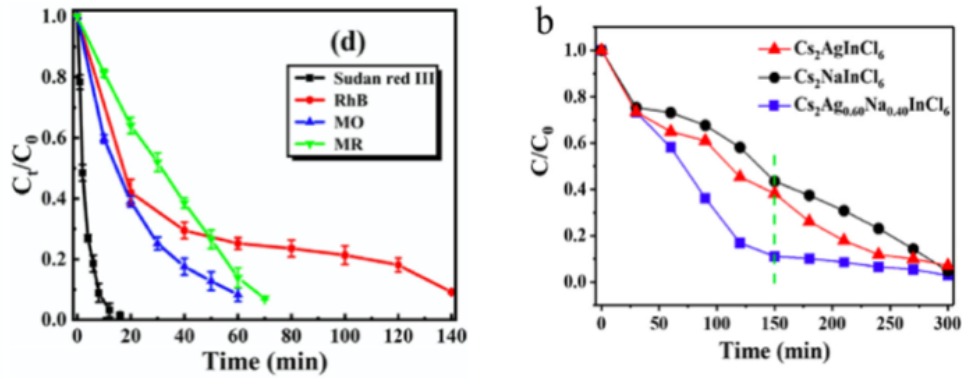


Figure 9: Degradation of organic dyes by (d)  $Cs_2AgInCl_6$  and (b)  $Cs_2Ag_{(1-x)}Na_xInCl_6$  [38] [64]

As discussed earlier, the presence of organic dyes in wastewater from various industries poses a concerning hazard, both to humans and the environment. These dyes are, in most cases, resistant to conventional wastewater treatment methods and can persist in the environment for a long time due to their complex structures, causing ecological disruption.

The phenomenon of Photocatalysis offers a promising solution for the degradation of these pollutants by using light to activate a semiconductor catalyst that decomposes the dye molecules into smaller and smaller parts. One material gaining traction in photocatalytic research is the double halide perovskite  $Cs_2AgInCl_6$ , exhibiting potential for dye degradation.

As mentioned earlier, studies have shown that  $Cs_2AgInCl_6$  possesses suitable bandgap energy ( $Cs_2AgInCl_6$  is known to have a direct band gap of around 3.33 eV [38]) for visible light absorption, a crucial factor for efficient photocatalysis under natural sunlight irradiation [38]. However, inherent limitations like low stability in water restrict its practical application. As a counter to this, doping with appropriate elements has emerged as a promising approach for reasons stated in the previous sections. Many doped variants of  $Cs_2AgInCl_6$  have been and are currently ongoing research.

Sun et al. investigated the effect of Na-doping on  $Cs_2AgInCl_6$  for organic dye degradation, their findings suggest that Na-doping  $Cs_2Ag_{0.6}Na_{0.4}InCl_6$  improves photocatalytic activity [64] compared to pristine  $Cs_2AgInCl_6$ . This enhancement is linked to factors like suppressed recombination of photogenerated charge carriers and the introduction of new energy levels within the bandgap, facilitating efficient light absorption and promoting the degradation processes.

## 1.9 Aims and Objectives

Knowing all this the main objectives for the project include

1. Synthesis of the series  $Cs_2Ag_{(1-x)}Na_xInCl_6$  for different values of x
2. Characterization of synthesized compound using XRD and SEM
3. Photodegradation of organic dye like methyl orange using the synthesized compound

## 2 Synthesis

### 2.1 Materials

- Hydrochloric Acid ( $HCl$ , 37 wt%)  
Acipur solution, manufactured by Loba Chemie
- Cesium Chloride ( $CsCl$ , 99.9%)  
Manufactured by Alfa Aesar  
Formula weight: 168.36
- Indium (III) Chloride ( $InCl_3$ , 99.9%)  
Manufactured by Aldrich  
Formula weight: 221.18
- Silver Chloride ( $AgCl$ , 99.9%)  
Manufactured by Alfa Aesar  
Formula weight: 143.32
- Sodium Chloride ( $NaCl$ , 99.9%)  
Manufactured by Sigma Aldrich  
Formula weight: 58.44



Figure 10: Precursor materials used in synthesis

All the precursors are used as received without any further purification.

## 2.2 Synthesis Process

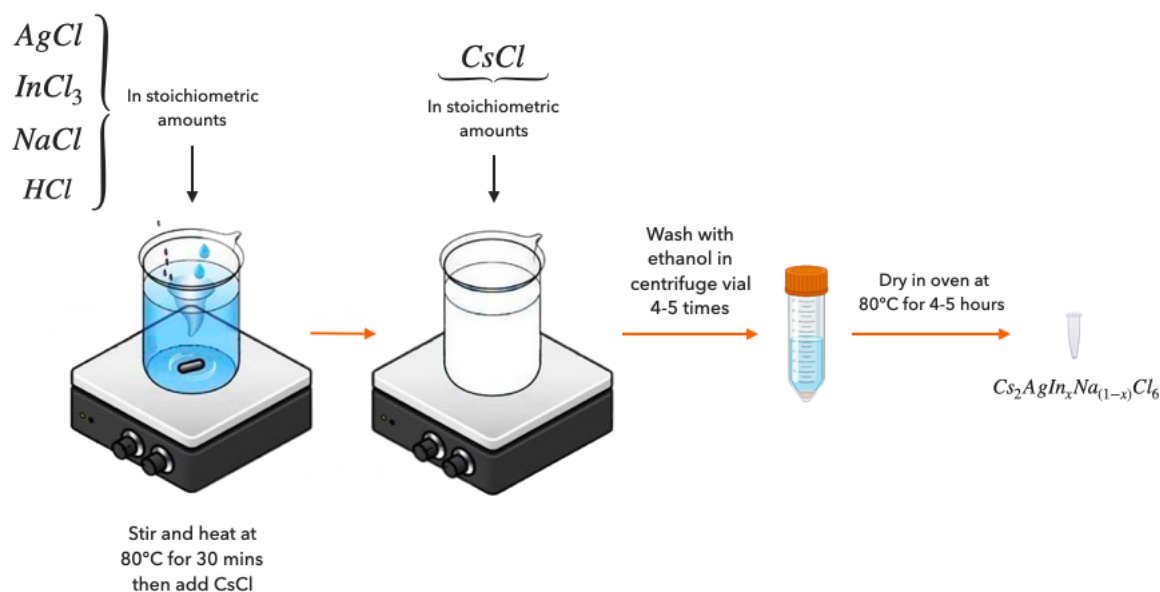


Figure 11: Schematic diagram of the process of Acid Precipitation synthesis

The series  $Cs_2Ag_{(1-x)}Na_xInCl_6$  was prepared using acid precipitation using the following reactants,

- $CsCl$  (99.9% pure Alfa-Aesar),
- $AgCl$  (99.9% pure Alfa-Aesar),
- $InCl_3$  (99.9% pure Aldrich)
- $NaCl$  (99.9% pure, Aldrich)

### 2.2.1 Procedure

- In stoichiometric ratios. The reactants undergo the following reaction in 37%  $HCl$  which was used as the solvent to facilitate the reaction.
- Calculated amounts of  $AgCl$  was weighed and added in a beaker.  $HCl$  was then added and the chunks of  $AgCl$  were broken down using a glass rod
- The mixture was heated and stirred using a magnetic stirrer at 75C. Calculated amount of  $NaCl$  was then added to it after 20 mins, Calculated amount of  $InCl_3$  was added in
- After 30 minutes calculated amount of  $CsCl$  was added in.
- As soon as  $CsCl$  was added to the mixture a white precipitate was formed. This was further stirred for thirty minutes.
- The contents were then collected in a centrifuge tube, washed in ethanol and centrifuged four times to remove any  $HCl$ .
- The contents were then collected in a beaker and The precipitate was then dried in ethanol in an oven at 90 C for an hour to get a powdered sample
- This powder was then ground using an agate mortar and pestle and collected for characterization and other studies.



a.



b.



c.

Figure 12: Figures shown: fig a.stirring process,figs b,c.Sample after drying

### 3 Characterization

Characterization of materials is the process of analyzing and understanding the structure and properties of materials at different scales, from atoms to macroscopic features. It is an essential part of materials science and engineering, as it reveals the relationship between the composition, morphology, and performance of materials.

Characterization is vital for development of good quality materials. The complete characterization of any material consists of phase analysis, structural and compositional characterization, micro-structural analysis and spectroscopic analysis. One single technique is not capable of providing complete characterization of a solid. In this chapter different analytical instrumental techniques are discussed which were used to characterize the samples prepared. There are many such methods of characterization, the ones required for this project are XRD, more precisely PXRD and UV Vis Spectroscopy

#### 3.1 X-Ray Diffraction (XRD)

X-ray diffraction (XRD) is a non-destructive analytical characterization technique that provides detailed information about the internal structure of crystalline substances, like lattice parameters, atomic arrangement, grain size, imperfections etc [12]

##### 3.1.1 Principle of XRD

XRD is based on the wave-particle duality principle. When a monochromatic X-ray beam interacts with a crystal, the incident X-rays are diffracted by the crystal lattice. The diffraction occurs due to the interference of the scattered waves. The is constructive interference, governed by Bragg's law, results in peak intensities known as reflections [50].

##### 3.1.2 Working of XRD

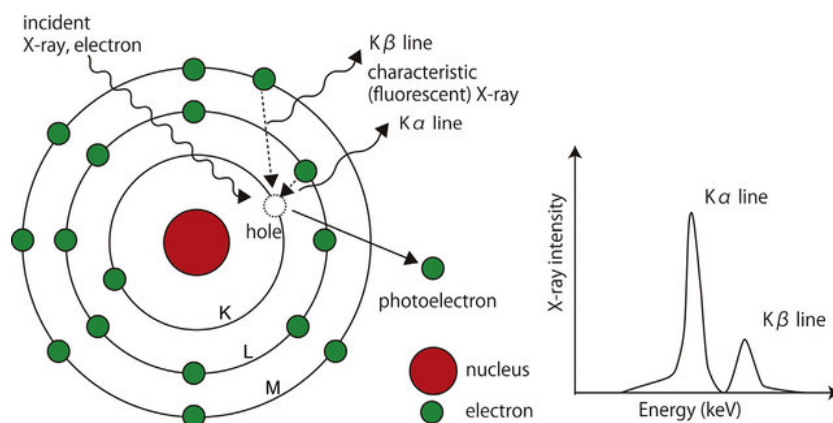


Figure 13: Generation of  $CuK\alpha$  radiaton and X Ray spectrum of Cu [67]

In an XRD, a monochromatic X-ray beam is incident on the sample. The X-rays are diffracted by the crystal lattice planes in the sample, diffracted X-rays are then detected, processed and counted. By scanning the sample through a range of  $2\theta$  angles, all possible diffraction directions of the lattice should be attained due to the random orientation of the powdered material. Conversion of the diffraction peaks to d-spacings allows identification of the mineral because each mineral has a set of unique d-spacings.

##### 3.1.3 Advantages and Disadvantages of XRD

- Advantages XRD offers several advantages, it is non-destructive in nature, rapid, has quantitative capabilities, and versatility. It can provide precise information about interatomic spacing, angles, and orientations of planes in a crystal and reveal irregularities in the crystal structure.
- Disadvantages Despite its advantages, XRD has some limitations. It requires a significant amount of sample, and the sample preparation can be challenging for certain materials. Also, XRD may not be suitable for samples with small crystallites or amorphous materials.

### 3.1.4 Single Crystal XRD vs Powder XRD

Single Crystal XRD and Powder XRD are two different methods of XRD, each with its own advantages and applications.

- Single Crystal XRD

Uses a single crystal as a sample. It provides detailed information about the atomic structure of a crystal. It can determine the exact atomic positions, thermal vibrations, electron density distribution, and other structural parameters. However, it requires a high-quality single crystal, which can be difficult to obtain for some materials.

- Powder XRD

Uses powdered material as sample. It is used for the analysis of polycrystalline materials and provides information about the phase composition and crystallinity of the sample. It is a bulk characterization technique and does not require a single crystal. However, it cannot provide detailed atomic structure information [59].

### 3.1.5 Interaction of X-rays with matter

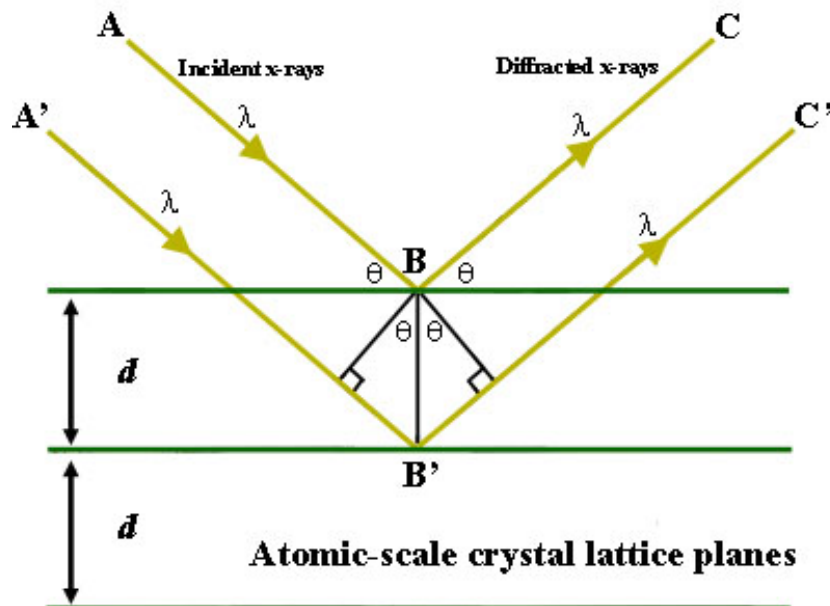


Figure 14: Bragg's Law reflection. The diffracted X-rays exhibit constructive interference when the distance between paths ABC and A'B'C' differs by an integer number of wavelengths ( $\lambda$ ) [16]

Bragg's approach to diffraction is to regard the crystals as built up in layers or planes and each of these layers or planes acts as a semi-transparent mirror. When X-rays with wavelength similar to atomic spacings are incident upon a crystalline material, some of the x-rays are reflected off the plane with an incidence equal to angle of reflection and the rest are transmitted to be subsequently reflected by succeeding planes.

Bragg's Law

$$n\lambda = 2d \sin \theta \quad (1)$$

where:

- $n$  is the order of diffraction, which is an integer. This refers to the number of wavelengths by which the path of the diffracted wave differs from the path of the incident wave.
- $\lambda$  is the wavelength of the incident X-ray beam.
- $d$  is the interplanar spacing, i.e., the distance between adjacent planes in the crystal lattice.
- $\theta$  is the angle of incidence of the X-ray beam with respect to the crystal lattice plane.

The physical interpretation of Bragg's Law is based on the concept of wave interference. When an X-ray beam is incident on a crystal lattice, it gets scattered by the atoms in the lattice. The scattered waves can interfere constructively or destructively, depending on their phase difference. For constructive interference (which leads to a peak in the diffracted X-ray intensity), the path difference between the waves scattered by two adjacent planes must be an integer multiple of the wavelength. So when Bragg's law is satisfied, the reflected beams are in phase and they interfere constructively. For angles other than Bragg's angle, they are out of phase and interfere destructively. Bragg's law imposes a strict condition on the angles at which reflection may occur [59].

### 3.1.6 Powder XRD

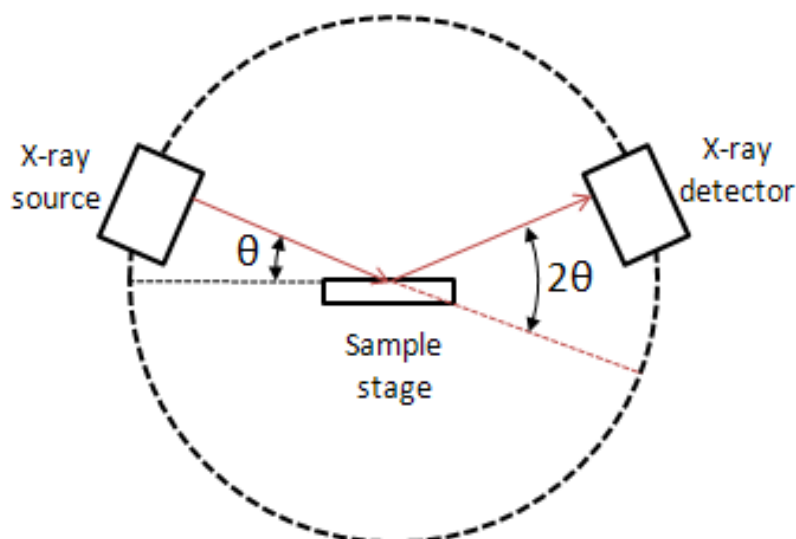


Figure 15: Formation of the cone of a diffracted beam. Adopted from reference [70]

X-ray Powder Diffraction (XRD) is a rapid analytical method utilized for identifying the phase of crystalline substances, and it can provide information about the dimensions of the unit cell, bulk composition, lattice parameters, particle size and purity of the sample. The material under analysis is thoroughly pulverized and homogenized to determine the average composition of the bulk.

In Powder X Ray Diffractometer, X-rays which are electromagnetic radiation having wavelength around  $1\text{ \AA}$  are produced when high energy particles such as electrons are accelerated through high potential to collide with target material. The resulting X-ray spectra usually have two components: a broad spectrum of wavelengths known as white radiation and a number of fixed or monochromatic wavelengths [6].

X-rays which are used in X Ray diffractometers are monochromatic X-rays. A beam of electrons when accelerated through high potential differences are allowed to strike a metal target such as Cu. The incident electron beam has sufficient energy to ionize some of the Cu K shell electrons. An electron in the outer orbit (such as L, M) can fill the vacancy created in the K shell and the energy released in the transition appears as X-radiation. For Cu, transition from L-shell to K shell appears as  $K\alpha$  radiation and transition from M-shell to K-shell appears as  $K\beta$  radiation.

### 3.1.7 Powder XRD method

In this method, a monochromatic beam of x-rays strikes a finely powdered sample in which there is random orientation of crystals in every possible direction. In such powdered samples, various planes are also present in every possible orientation. For each set of planes, at least some crystals must be oriented in at Bragg's angle, to the incident beam and thus Bragg's law is satisfied for those crystals and planes.

The diffracted beam is then detected by the detector. For any set of lattice planes, the diffracted radiation from the surface of a cone. The only requirement for diffraction is that the planes should be at Bragg's angle with respect to the incident beam and no restriction is placed on the angular orientation of the planes about the axis of the incident beam. In a finely powdered sample, crystals are present at every possible angular position about the incident beam so the diffracted radiation appears to be emitted from the sample as cones of radiation. Each set of planes gives its own cone of radiation [6][59].

### 3.1.8 Powder X-ray Diffractometer

Powder X-ray Diffractometer consists of following components:

- X-ray Source: High energy electrons are produced from heated tungsten filament and this is allowed to impinge on small metal target example Copper in a sealed diffraction tube.
- Collimator: X-rays are generated by target material and then it passes through the collimator. It consists of a set of two metal plates which are closely packed and separated by a small distance. The collimator absorbs all the x-rays except the narrow beam that passes through it.
- Monochromators: Monochromators separate polychromatic light into a range of individual wavelengths. Graphite Monochromator is used in Rigaku SmartLab X-ray diffractometer. The graphite monochromator optimizes sensitivity by lowering the background level. It improves signal-to-noise by eliminating fluorescence from Co, Ni, Fe, Mn containing materials.
- Filters: Filters absorb undesirable radiations but allow the radiation of desired wavelength to pass. Example nickel filter is used to remove  $K\beta$  radiations of copper. These filters are used as an alternative to monochromators.
- Detector: The D/TEX Ultra 250 is used to detect the diffracted beam in Rigaku Smart lab powder X-ray diffractometer. It is a 1D Silicon strip detector that decreases data acquisition time by 50% compared to competitive detectors. This is achieved by increasing the active area of the aperture and thus increasing the count rate. D/TEX ultra has smaller pixel pitch and longer in direction of  $2\theta$  [54].

### 3.1.9 Applications

X-ray powder diffraction is most widely used for the identification of unknown crystalline materials (e.g. minerals, inorganic compounds). Determination of unknown solids is critical to studies in geology, environmental science, material science, engineering and biology[6].

Other applications include:

- characterization of crystalline materials
- identification of fine-grained minerals such as clays and mixed layer clays that are difficult to determine optically
- determination of unit cell dimensions
- measurement of sample purity
- Determine crystal structures using Rietveld refinement
- Determine of modal amounts of minerals (quantitative analysis) characterize thin films samples by:
  - Determining lattice mismatch between film and substrate and to inferring stress and strain
  - Determining dislocation density and quality of the film by rocking curve measurements
  - Measuring superlattices in multilayered epitaxial structures
  - Determining the thickness, roughness and density of the film using glancing incidence X-ray reflectivity measurements
  - Make textural measurements, such as the orientation of grains, in a polycrystalline sample.

### 3.1.10 Advantages and disadvantages of X-ray Powder Diffraction (XRD)

- Strengths Powerful and rapid ( $\approx 20$  min) technique for identification of an unknown mineral In most cases, it provides an unambiguous mineral determination Minimal sample preparation is required XRD units are widely available Data interpretation is relatively straight forward
- Limitations Homogeneous and single phase material is best for identification of an unknown Must have access to a standard reference file of inorganic compounds (d-spacings, hkl's) Requires tenths of a gram of material which must be ground into a powder For mixed materials, detection limit is  $\approx 2\%$  of sample For unit cell determinations, indexing of patterns for non-isometric crystal systems is complicated Peak overlay may occur and worsens for high angle 'reflections'



Figure 16: Rigaku Smart Lab Powder X-ray diffractometer at ULMC of Goa University.

## 3.2 Ultraviolet-visible (UV-Vis) spectroscopy

Ultraviolet-visible (UV-Vis) spectroscopy is a type of absorption spectroscopy that measures the amount of UV and visible light absorbed by a sample. It is widely used to identify and quantify compounds in various samples.

### 3.2.1 The principle of UV

UV-Vis spectroscopy is an analytical technique that measures the amount of discrete wavelengths of UV or visible light that are absorbed by or transmitted through a sample in comparison to a reference or blank sample. This property is influenced by the sample composition, potentially providing information on what is in the sample and at what concentration. Since this spectroscopy technique relies on the use of light, let's first consider the properties of light.

Light has a certain amount of energy which is inversely proportional to its wavelength. Thus, shorter wavelengths of light carry more energy and longer wavelengths carry less energy. A specific amount of energy is needed to promote electrons in a substance to a higher energy state which we can detect as absorption. Electrons in different bonding environments in a substance require a different specific amount of energy to promote the electrons to a higher energy state.

This is why the absorption of light occurs for different wavelengths in different substances. Humans are able to see a spectrum of visible light, from approximately 380 nm, which we see as violet, to 780 nm, which we see as red. UV light has wavelengths shorter than that of visible light to approximately 100 nm. Therefore, light can be described by its wavelength, which can be useful in UV-Vis spectroscopy to analyze or identify different substances by locating the specific wavelengths corresponding to maximum absorbance [51][57].

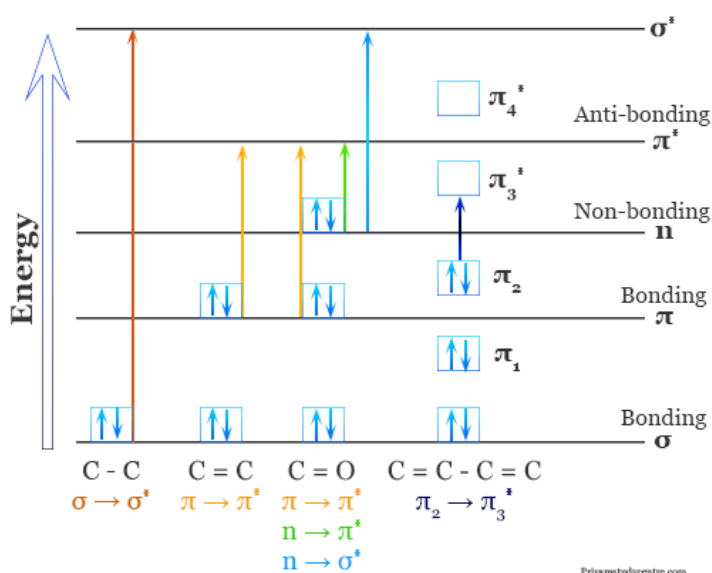


Figure 17: Electronic transitions in UV-Visible spectroscopy.[73]

A compound appears coloured if it selectively absorbs light from the visible region. The absorbed energy raises the molecule from ground energy state ( $E_0$ ) to higher excited energy state ( $E_1$ ).

$$\Delta E = E_1 - E_0 = h\nu = h\left(\frac{c}{\lambda}\right)$$

The difference in energy  $\delta E$  depends on how tightly the electrons are bound to the bonds, and accordingly absorption will occur in UV or visible range. In compounds having sigma bonds, the electrons in the molecule are tightly bound so radiation from the UV region will be absorbed. No absorption occurs in the visible region, so the compound appears colourless. If the electrons in the molecule are loosely bound, absorption occurs in the visible region and the compound appears coloured.

There are three types of ground state orbitals in molecules:

- $\sigma$ (bonding) molecular orbital – Electrons in this orbital are tightly bound and require high energy for their excitation and thus don't show absorption near the UV region.

- $\pi$ (bonding) molecular orbital – Electrons in this orbital are found in multiple bonds and are generally mobile. Since  $\pi$  bonds are weak, the energy produced by UV radiation can excite its electrons from ground level to higher energy levels.
- n (non-bonding) molecular orbital – Valence electrons which do not participate to form a chemical bond in a molecule are called non-bonding electrons or n electrons. These are generally lone pairs of electrons and can be excited by UV radiation. Besides these, the anti-bonding orbitals are  $\sigma$  orbital and  $\pi$  orbital.

### 3.2.2 Beer-Lambert Law

The Beer-Lambert law, often used in UV-Visible spectroscopy, is a fundamental principle that relates the attenuation of light to the properties of the material through which the light is traveling. A light beam is emitted via source and the incident beam passes through the sample and the wavelength of light reaching the detector is measured. The measured wavelength provides qualitative and quantitative information about the loaded sample such as chemical structure and number of molecules present. The information can be obtained as absorbance, transmittance or reflectance of radiation of range 160 nm to 3500 nm. When a light beam of specific energy (intensity) is focused onto a sample, the molecules absorb some energy of the incident light. A photodetector measures the intensity of light coming out of the sample and registers its absorbance. The absorption or transmission spectra of the light absorbed or transmitted by the sample against the wavelength is recorded. Beer-Lambert Law is the basic principle of quantitative analysis which states that absorbance of light by the sample is directly proportional to analyte concentration and optical path length.

$$A = \epsilon \cdot l \cdot c \quad (2)$$

where:

- $A$  is the absorbance,
- $\epsilon$  is the molar absorptivity or molar extinction coefficient,
- $c$  is the concentration of the solution, and
- $l$  is the path length of the light.

This law implies that the absorbance is directly proportional to both the concentration of the substance in the solution and the path length of the light. The molar absorptivity,  $\epsilon$ , is a measure of the probability of the electronic transition.

Transmittance (T) is given by

$$T = \frac{I}{I_0} \quad (3)$$

Where  $I$  is intensity of incident light and  $I_0$  is the intensity of light detected and absorbance is the inverse of transmittance given by

$$A = \log_{10}\left(\frac{I_0}{I}\right) = \epsilon l c \quad (4)$$

the Beer-Lambert law is crucial because it allows for the determination of the concentration of a sample based on its absorbance. However, it's important to note that there can be deviations from the Beer-Lambert law due to factors such as chemical interactions, changes in refractive index, and light scattering etc [?].

### 3.2.3 Instrumentation

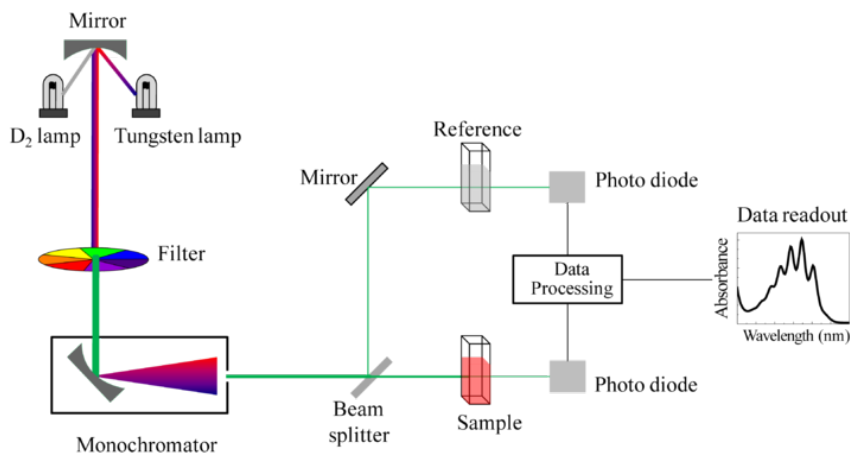


Figure 18: Schematic diagram of UV- visible spectrophotometer.[10]

UV-visible spectrometry, is a method used to measure the absorbance of light by a sample in the ultraviolet to visible range (approx 200 - 800 nm).

The instrumentation of a UV-visible spectrometer can be broken down into four main components:

- **Light Source:** The light source is typically a deuterium lamp for the UV region (190 - 380 nm) which produces continuous UV spectrum by electrically exciting deuterium or hydrogen at low pressures and a tungsten halogen lamp for the visible region (380 - 800 nm). These lamps emit a broad spectrum of light, covering the entire range of interest.
- **Monochromator:** The monochromator is used to isolate a narrow band of wavelengths from the broad spectrum produced by the light source. This is typically achieved using a diffraction grating, which disperses the light into its component wavelengths. The desired wavelength is then selected using a slit.
- **Sample Holder:** The sample holder, or cuvette, holds the sample solution. It is typically made of quartz or some other material that is transparent to UV and visible light.
- **Detector:** The detector measures the intensity of the light that passes through the sample. The most common type of detector is a photodiode or a photomultiplier tube, which generates an electrical current proportional to the intensity of the light.

The operation of a UV-visible spectrometer involves directing the light from the light source through the monochromator and onto the sample.

Before reaching the sample, the light is divided into two parts of similar intensity with a half mirror splitter. One part travels via a cuvette having a solution of material to be examined in a transparent solvent and the second beam or reference beam travels through a cuvette having only solvent.

The detector detects the intensity of light transmitted by both the cuvettes and sends that data to a meter to record and display the values. Electronic detectors calculate and compare the intensities of the light beams [51].

### 3.2.4 Working

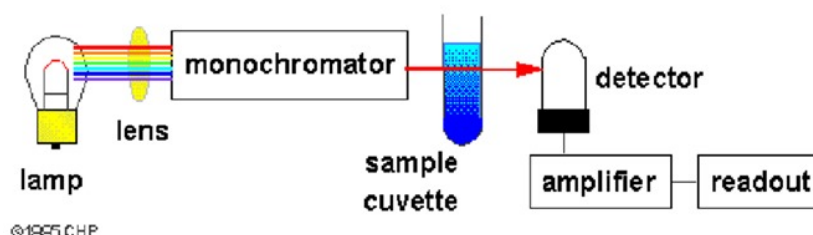


Figure 19: Simple Schematic diagram of UV- visible spectrophotometer.[1]

There exist many variations on the UV-Vis spectrophotometer and the specific details of the instrumentation can vary between different models and manufacturers of UV-visible spectrometers.

To gain a better understanding of how an UV-Vis spectrophotometer works, let us consider the main components, depicted in Figure .

A simplified schematic of the main components in a UV-Vis spectrophotometer. The path of light from the light source, to the wavelength selector, sample and detector prior to signal processing is shown.

- Light source: As a light-based technique, a steady source able to emit light across a wide range of wavelengths is essential. A single xenon lamp is commonly used as a high intensity light source for both UV and visible ranges. Xenon lamps are, however, associated with higher costs and are less stable in comparison to tungsten and halogen lamps.

For instruments employing two lamps, a tungsten or halogen lamp is commonly used for visible light, whilst a deuterium lamp is the common source of UV light.

As two different light sources are needed to scan both the UV and visible wavelengths, the light source in the instrument must switch during measurement. In practice, this switchover typically occurs during the scan between 300 and 350 nm where the light emission is similar from both light sources and the transition can be made more smoothly.

Wavelength selection: In the next step, certain wavelengths of light suited to the sample type and analyte for detection must be selected for sample examination from the broad wavelengths emitted by the light source. Available methods for this include:

- Monochromators - A monochromator separates light into a narrow band of wavelengths. It is most often based on diffraction gratings that can be rotated to choose incoming and reflected angles to select the desired wavelength of light.<sup>1,2</sup> The diffraction grating's groove frequency is often measured as the number of grooves per mm. A higher groove frequency provides a better optical resolution but a narrower usable wavelength range. A lower groove frequency provides a larger usable wavelength range but a worse optical resolution. 300 to 2000 grooves per mm is usable for UV-Vis spectroscopy purposes but a minimum of 1200 grooves per mm is typical. The quality of the spectroscopic measurements is sensitive to physical imperfections in the diffraction grating and in the optical setup. As a consequence, ruled diffraction gratings tend to have more defects than blazed holographic diffraction gratings.<sup>3</sup> Blazed holographic diffraction gratings tend to provide significantly better quality measurements.
- Absorption filters - Absorption filters are commonly made of colored glass or plastic designed to absorb particular wavelengths of light.
- Interference filters - Also called dichroic filters, these commonly used filters are made of many layers of dielectric material where interference occurs between the thin layers of materials. These filters can be used to eliminate undesirable wavelengths by destructive interference, thus acting as a wavelength selector.
- Cutoff filters - Cutoff filters allow light either below (shortpass) or above (longpass) a certain wavelength to pass through. These are commonly implemented using interference filters.
- Bandpass filters -Bandpass filters allow a range of wavelengths to pass through that can be implemented by combining shortpass and longpass filters together.

- Monochromators are most commonly used for this process due to their versatility. However, filters are often used together with monochromators to narrow the wavelengths of light selected further for more precise measurements and to improve the signal-to-noise ratio.
- Sample analysis: Whichever wavelength selector is used in the spectrophotometer, the light then passes through a sample. For all analyses, measuring a reference sample, often referred to as the "blank sample", such as a cuvette filled with a similar solvent used to prepare the sample, is imperative. If an aqueous buffered solution containing the sample is used for measurements, then the aqueous buffered solution without the substance of interest is used as the reference. When examining bacterial cultures, the sterile culture media would be used as the reference. The reference sample signal is then later used automatically by the instrument to help obtain the true absorbance values of the analytes.

It is important to be aware of the materials and conditions used in UV-Vis spectroscopy experiments. For example, the majority of plastic cuvettes are inappropriate for UV absorption studies because plastic generally absorbs UV light. Glass can act as a filter, often absorbing the majority of UVC (100-280 nm)<sup>2</sup> and UVB (280-315 nm) but allowing some UVA (315-400 nm) to pass through.

Therefore, quartz sample holders are required for UV examination because quartz is transparent to the majority of UV light. Air may also be thought of as a filter because wavelengths of light shorter than about 200 nm are absorbed by molecular oxygen in the air.

A special and more expensive setup is required for measurements with wavelengths shorter than 200 nm, usually involving an optical system filled with pure argon gas. Cuvette-free systems are also available that enable the analysis of very small sample volumes, for example in DNA or RNA analyses.

- Detection: After the light has passed through the sample, a detector is used to convert the light into a readable electronic signal. Generally, detectors are based on photoelectric coatings or semiconductors.

A photoelectric coating ejects negatively charged electrons when exposed to light. When electrons are ejected, an electric current proportional to the light intensity is generated. A photomultiplier tube (PMT)<sup>4</sup> is one of the more common detectors used in UV-Vis spectroscopy. A PMT is based on the photoelectric effect to initially eject electrons upon exposure to light, followed by sequential multiplication of the ejected electrons to generate a larger electric current. PMT detectors are especially useful for detecting very low levels of light [11][69].

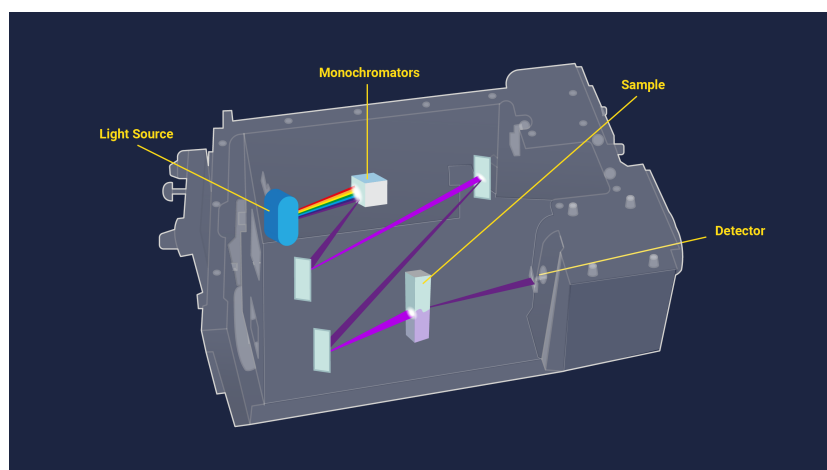


Figure 20: Schematic diagram of a cuvette-based UV-Vis spectroscopy system.[14]

When semiconductors are exposed to light, an electric current proportional to the light intensity can pass through. More specifically, photodiodes and charge-coupled devices (CCDs)<sup>7</sup> are two of the most common detectors based on semiconductor technology. After the electric current is generated from whichever detector was used, the signal is then recognized and output to a computer or screen. UV-Vis spectroscopy information may be presented as a graph of absorbance, optical density or transmittance as a function of wavelength. However, the information is more often presented as a graph of absorbance on the vertical y axis and wavelength on the horizontal x axis.

Based on the UV-Vis spectrophotometer instrumentation reviewed in the previous subsection of this article, the intensity of light can be reasonably expected to be quantitatively related to the amount of light absorbed

by the sample. The absorbance ( $A$ ) is equal to the logarithm of a fraction involving the intensity of light before passing through the sample  $I_0$  divided by the intensity of light after passing through the sample ( $I$ ). The fraction  $I$  divided by  $I_0$  is also called transmittance ( $T$ ), which expresses how much light has passed through a sample. However, Beer–Lambert’s law is often applied to obtain the concentration of the sample ( $c$ ) after measuring the absorbance ( $A$ ) when the molar absorptivity ( $\epsilon$ ) and the path length ( $L$ ) are known.

Typically,  $\epsilon$  is expressed with units of  $Lmol^{-1}cm^{-1}$ ,  $L$  has units of cm, and  $c$  is expressed with units of  $molL^{-1}$ . As a consequence,  $A$  has no units. Sometimes AU is used to indicate arbitrary units or absorbance units but this has been strongly discouraged.

For data analysis, the graph of absorbance versus concentration can indicate how sensitive the system is when building a calibration curve. When a linear least squares regression equation is used, the slope from the line of best fit indicates sensitivity. If the slope is steeper, the sensitivity is higher. Sensitivity is the ability to differentiate between the small differences in the sample concentration. From Beer–Lambert’s Law, the sensitivity can be partially indicated by the molar absorptivity  $\epsilon$ . Knowing the values beforehand, if available, can help to determine the concentrations of the samples required, particularly where samples are limited or expensive.

For reliability and best practice, UV-Vis spectroscopy experiments and readings should be repeated. When repeating the examination of a sample, in general, a minimum of three replicate trials is common, but many more replicates are required in certain fields of work. A calculated quantity, such as the concentration of an unknown sample, is usually reported as an average with a standard deviation. Reproducible results are essential to ensure precise, high quality measurements. Standard deviation, relative standard deviation, or the coefficient of variation help to determine how precise the system and measurements are. A low deviation or variation indicates a higher level of precision and reliability.

### 3.3 Scanning Electron Microscopy (SEM)

SEM is a type of electron microscope that produces images of a sample by scanning the surface with a focused beam of electrons<sup>1</sup>. The SEM allows scientists to observe materials at length scales that are too small for visible light [18]. It can determine microstructure, morphology, and elemental composition of electrically conductive samples. SEMs can have a resolution as low as 1 nm (over 100,000x magnification), although the resolution is not as good as TEM (Transmission Electron Microscopy) which can even detect columns of atoms [21].

#### 3.3.1 Principle of SEM

The Scanning electron microscope works on the principle of applying kinetic energy to produce signals on the interaction of the electrons. These electrons are secondary electrons, backscattered electrons, and diffracted backscattered electrons which are used to view crystallized elements and photons.

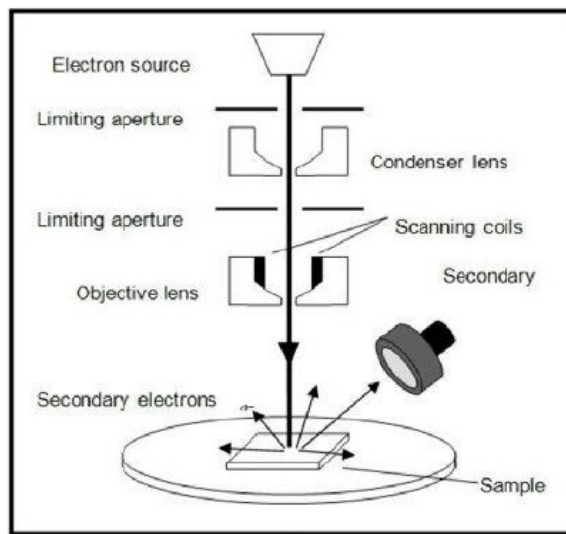


Figure 21: Simple Schematic diagram of SEM.[45]

- Backscattered electrons: Backscattered electrons are reflected back when the primary electron beams the sample. These are elastic interactions. Backscattered electrons come from deeper areas of samples. Its image displays high sensitivity in difference in atomic numbers which will show up as brighter or darker
- Secondary electrons: The secondary electrons are from atoms of the sample and they are inelastic interactions. It comes from surface regions. Scattered electrons give information about the nano and micro structure of the samples in the form of an image.

Scintillator is used as a detector which is held at a high positive potential of several KV and the secondary electrons are accelerated into the scintillator to give visible light which is then detected by photomultiplier. At each point signals are emitted from specimens and are collected by detectors. The detector signal is synchronized with the known location of the beam on the specimen and signal intensity used to modulate the corresponding image pixel. The signals collected in series are combined to form an Image whose dimension distribution depends upon the scan pattern chosen [18].

### 3.3.2 Instrumentation

The scanning electron microscope instrument consists of the following components [58]:

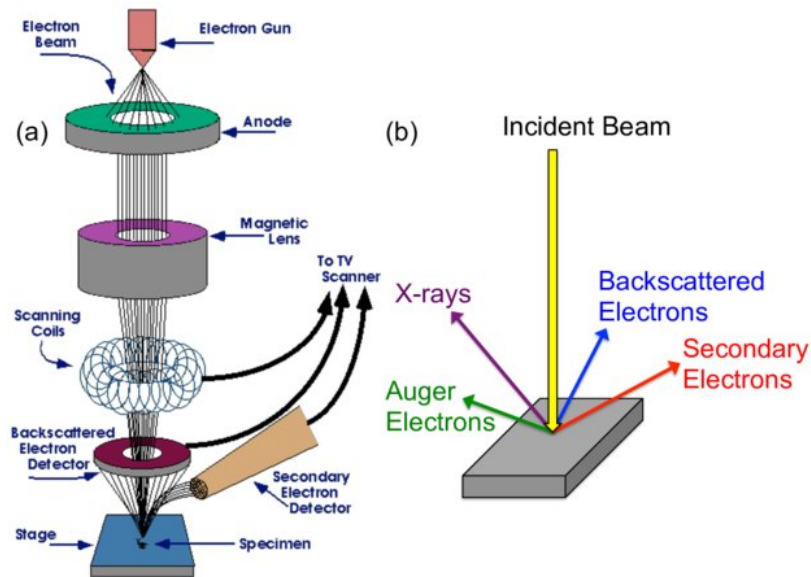


Figure 22: Simple Schematic diagram of SEM.[58]

- Electron source: The electron source generates electrons at top of the microscope column. The electrons are emitted by heated filament of Tungsten or Lanthanum Hexabromide by thermionic emission.
- Anode: Anode has a positive charge, which attracts the electrons to form an electron beam.
- Magnetic lens: Magnetic lens controls the size of the beam and determines the number of electrons in the beam. The size of the beam will decide the resolution of the image. Apertures can be also used to control the size of the image.
- Scanning coils: The scanning coils deflect the electrons along x and y axes. To ensure it scans in a raster fashion over the surface of the sample.
- Objective lens: The objective lens is the last lens among lenses that creates the electron beam.

Since this lens is very close to the sample, it focuses the beam to a very small spot on the sample. Since electrons cannot pass through glass, SEM glass is electromagnetic. They are made up of coils of wire inside metal poles. When current passes through these coils, they generate magnetic fields. Since electrons are highly sensitive to magnetic field which allows the lenses in the microscope to control them [21].

### 3.3.3 Advantages and disadvantages of SEM

Scanning electron microscopy has a broad range of research and practical applications[27].It provides detailed, topographical images, providing versatile data.Given proper training, SEM equipment is straightforward to operate, and specialist but user-friendly software supports it. Modern SEM data comes in digital form.It is a rapid process, and instruments can complete analysis in under five minutes.There is a degree of sample preparation necessary, but usually this is minimal.

Scanning Electron Microscopy (SEM) has several advantages and disadvantages:

- Advantages:
  - High Resolution: SEM provides digital image resolution as low as 15 nanometers, which is beneficial for characterizing microstructures such as fracture, corrosion, grains, and grain boundaries1.
  - Traceable Standard for Magnification: All imaging is calibrated to a traceable standard, making it easy to apply analysis to saved images1.

- Chemical Analysis: SEM with Energy Dispersive Spectroscopy (EDS) provides qualitative elemental analysis, standardless quantitative analysis, X-ray line scans, and mapping.
- Large Depth of Field: More of a specimen can be in focus at one time.
- 3D Imaging: SEM allows the external, 3D structure of specimens to be observed.
- Disadvantages:
  - Vacuum Environment: SEM samples must be solid and vacuum-compatible<sup>1</sup>. However, higher pressures can be used for imaging of vacuum-sensitive samples that are nonconductive and volatile.
  - Lower Resolution than TEM: SEMs give lower resolution images (less detail) than Transmission Electron Microscopes (TEMs).

### 3.3.4 Applications

SEM is a versatile tool for characterizing materials at high magnifications. It offers a wealth of information on size, shape, and composition on solid surfaces, magnifying to submicron and even hundreds of microns across. It does this by harnessing two key electron beam interactions[53]:

- Secondary electrons: these reveal topographic details with great contrast, ideal for visualizing surface features like textures, cracks, pores, and particle morphology.
- Back-scattered electrons: these provide compositional information based on the atomic number of elements, enabling differentiation between phases and identification of heavier elements within the material[49].

Its applications include

#### 1. Morphology and Surface Analysis:

- Fracture and failure analysis: SEM unveils information about crack propagation, grain boundaries, and potential failure mechanisms, guiding material selection and optimization for specific applications.
- Characterization of nanomaterials: SEM shines in the study of nanomaterials, providing high-resolution images of their intricate structures and morphologies, which is crucial for understanding their unique properties and behavior.
- Adhesion and interface analysis: Examining interfaces between different materials, SEM can reveal details about adhesion, morphology, and interdiffusion, which is essential for understanding material interactions and performance in composite structures or devices.

#### 2. Elemental Analysis:

- Energy-Dispersive X-ray Spectroscopy (EDS): Coupled with SEM, EDS offers localized elemental composition and chemical state information. This provides information on the identification of phases, contaminants, and elemental distribution, painting a clear picture of a material's composition and aiding in understanding its properties and performance [56].
- Mapping elemental distribution: SEM-EDS allows researchers to map the distribution of elements across a surface. This reveals compositional variations and potential segregation of dopants, providing valuable insights into material homogeneity and informing optimization strategies.

#### 3. Microstructural Analysis:

- Grain size and morphology: SEM can provide a lot of information on the grains within a material, revealing their size, shape, and orientation. This information directly impacts mechanical and electrical properties, guiding material processing and performance optimization.
- Phase identification and distribution: Differentiating between different phases present in a material, SEM reveals their morphology and distribution, providing crucial insights into the microstructure and performance of multiphase materials [15].

#### 4. In-situ and Operando Studies:

Dynamic observation of processes: Advanced SEM techniques enable researchers to observe materials undergoing dynamic processes like deformation, corrosion, or chemical reactions in real-time. This invaluable capability offers direct insights into material behavior under various conditions, informing material development and engineering efforts.



Figure 23: Carl Zeiss Scanning Electron Microscope at USIC of Goa University.

### 3.4 Photocatalysis

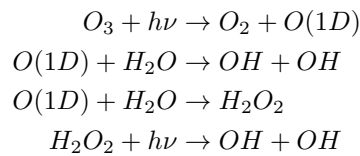
The term photocatalyst is a combination of two words: 'photo' related to 'photon' or 'light' and 'catalyst', which is a substance that alters the reaction rate with its presence. Therefore, photocatalysts are materials that change the rate of a chemical reaction on exposure to light. This phenomenon is known as photocatalysis. In essence, photocatalysis refers to the phenomenon where materials, primarily semiconductors, accelerate chemical reactions upon exposure to light [19].

This process hinges on the generation of electron-hole pairs within the semiconductor upon light absorption. These excited states fuel various chemical reactions, transforming reactants into desired products. All the while semiconductor itself remains unchanged throughout the reaction, acting as a true catalyst. These Photocatalytic reactions can be categorised into two types based on the physical state of the reactants

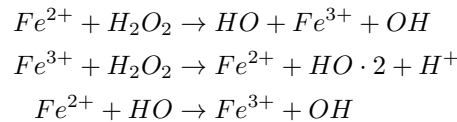
- **Homogeneous photocatalysis:**

where Both the catalyst and reactants are in a single phase. it can be used for reactions that occur in solution or in the gas phase such photocatalytic reactions are termed as homogeneous photocatalysis.

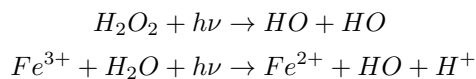
One of the very common examples of homogeneous photocatalysts used is ozone and photo-Fenton systems ( $Fe^{2+}$  and  $Fe^{2+}/H_2O_2$ ). Here the reactive species is to be the hydroxyl radical ( $OH$ ) which tends to be used for various purposes and objectives. This mechanism of producing hydroxyl radical ( $OH$ ) by ozone can follow these two paths mentioned below [36].



In the same way, the Fenton system ( $Fe^{2+}$ ) produce hydroxyl radical ( $\bullet OH$ ) by the mechanism shown below.



In the Photo-Fenton systems ( $Fe^{2+}$  and  $Fe^{2+}/H_2O_2$ ) type processes, supplemental sources of OH radicals are also considered: via photolysis of  $H_2O_2$ , and by the reduction of  $Fe^{3+}$  ions under UV light as follows:



The productivity and effectiveness of Fenton type processes is influenced by various operating parameters/variables such as concentration of hydrogen peroxide ( $H_2O_2$ ), pH as well as intensity of the UV light. The leading edge of this process is the capability of using sunlight with light sensitivity up to 450 nm, hence; saving the process from use of high costs of UV lamps and electrical energy.

These type of reactions in homogeneous photocatalysis are proved to be more convenient and economical than the other photocatalysis types, however the major downsides of this process are the low pH values, which are needed, because iron (Fe) precipitates at some higher pH values, furthermore the fact that iron (Fe) has to be eliminated after the treatment [36].

- **Heterogeneous photocatalysis:**

When the catalyst and reactants are in different phases. It is typically used for reactions that involve a solid semiconductor and a liquid or gas reactant. Such photocatalytic reactions are classified as heterogeneous photocatalysis.

In general and commonly used heterogeneous photocatalysts include transition metal oxides and semiconductors, which undergo unique characteristics. Contrary to the metals that possess a continuum of electronic states, semiconductors usually have ineffective energy regions where no such energy levels are available to develop rejoining of an electron and a hole produced by photo-activation in the solid substance.

The void/ineffective region, which outstretches from the top of the filled valence band to the bottom of the vacant conduction band, is termed as the band gap. The development of new and more efficient photocatalysts is an active area of research in materials science and chemistry, with the goal of finding sustainable and renewable solutions for energy production and environmental protection [36] [24].

### 3.4.1 Mechanism

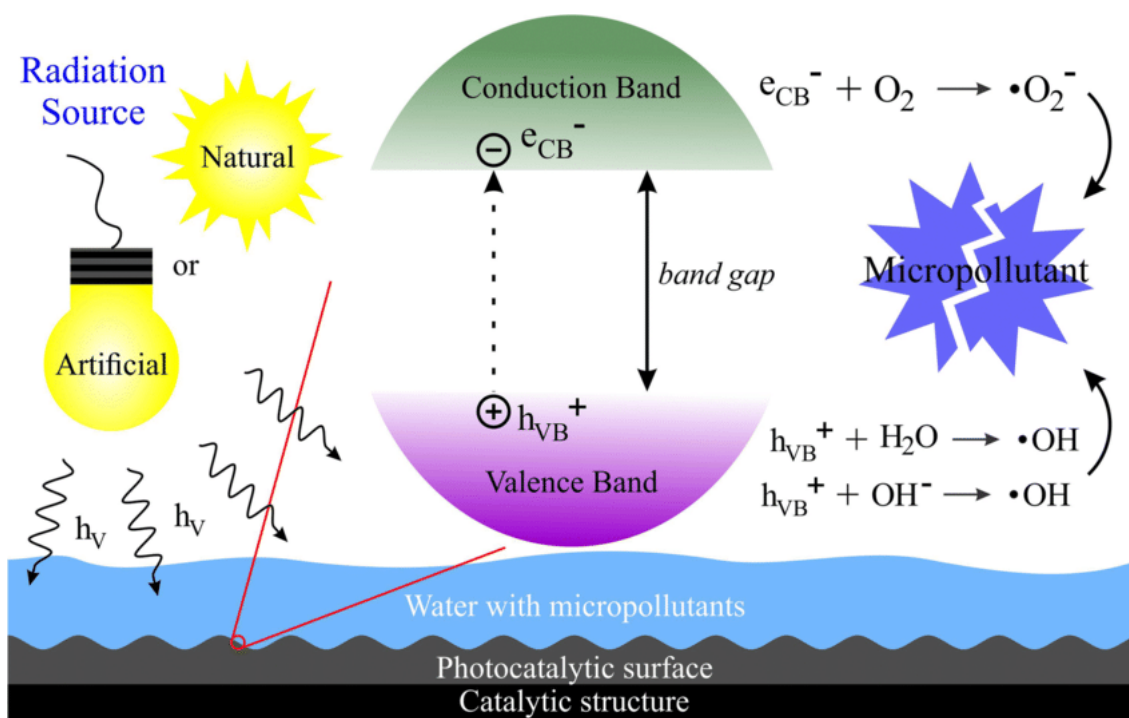


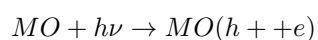
Figure 24: Schematic diagram of mechanism of photocatalysis [19]

The process of Photocatalysis can be used with a practical and successful approach in a real earth environment in order to decompose different types of pollutants, and it can enhance the quality of air in the atmosphere. Therefore the process of Photocatalysis can be used in the building and construction industry for the purpose of improving indoor air quality. In this process a photon with energy equal to or greater than that of the materials band gap is absorbed by the semiconductor used, then an electron excites from the valence band to the conduction band, so it generates a positive (+ve) hole in the valence band.

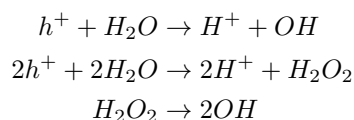
This phenomenon of photo-generated electron-hole pairs is called the exciton. The excited electron and hole can recombine or rejoin and release the energy that they gained when the electron was excited as heat. This Exciton and recombination is not desirable and the higher levels of it take the process to an ineffective photocatalyst. Because of this reason endeavors to flourish and develop functional photocatalysts frequently put an emphasize on extending the exciton lifetime, so that improving electron-hole separation using different approaches that usually depend upon structural characteristics such as phase hetero-junctions (for example; anatase-rutile interfaces), noble-metal nanoparticles, silicon nanowires and substitutional cation doping etc. The main objective of photocatalyst designing is to facilitate and pave the way for reactions between the excited electrons with oxidants to produce reduced products.

Additionally in order to make reactions between the holes generated along with the reductants to produce oxidized products. Because of the generation of positive (+ve) holes and electrons, redox reactions occur at the

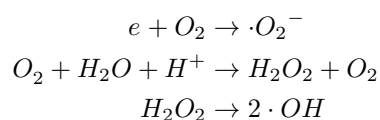
surface of semiconductors. The mechanism of the oxidative reaction shown below, depicts the positive holes that react with the moisture present on the material's (metal oxide) surface and produce a hydroxyl radical ( $OH$ ). This reaction begins with photo-induced exciton-generation in the metal oxide surface (where; MO stands for metal oxide):



Oxidative reactions due to photocatalytic effect are as below:



Reductive reactions due to photocatalytic effect are as below:



Finally, the generation of hydroxyl radical ( $OH$ ) takes place in both reactions mentioned above. Such hydroxyl radical ( $OH$ ) are extremely oxidative in nature and non-selective with redox potential of ( $E_0 = +3.06V$ ) as well.



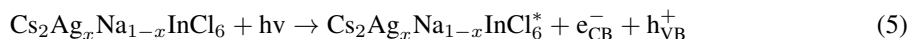
Figure 25: Photochemical Reactor at SPAS, Goa University

### 3.4.2 Photocatalytic Mechanism of $Cs_2Ag_{(1-x)}Na_xInCl_6$ .

The photocatalytic degradation of organic pollutants by your compound ( $Cs_2Ag_xNa_{1-x}InCl_6$ ) involves a series of light-induced reactions. Here, we discuss the key steps involved:

- Light Activation and Charge Separation

When irradiated with light of sufficient energy ( $h\nu$ ), electrons ( $e$ ) in the compound are excited from the valence band (VB) to the conduction band (CB), leaving behind holes ( $h^+$ ) in the VB. This process is represented by Equation 5:



- Redox Reactions and Dye Degradation

The excited electrons in the conduction band can react with dissolved oxygen ( $O_2$ ) molecules to generate superoxide radical anions ( $O_2^\bullet$ ), as shown in Equation 6. These superoxide radicals can further react with water molecules ( $H_2O$ ) to produce hydroperoxyl radicals ( $HO^\bullet$ ) and hydroxyl ions ( $OH^-$ ), as shown in Equation 7.



Alternatively, the holes in the valence band can directly react with hydroxyl ions ( $OH^-$ ) to form additional hydroxyl radicals ( $OH^\bullet$ ), as shown in Equation 8. In some cases, the holes can also directly participate in dye degradation, although this is a less frequent pathway (Equation 9).



The highly reactive hydroxyl radicals ( $OH^\bullet$ ) generated through these pathways are the primary oxidizing species responsible for the degradation of organic dye molecules. They attack the dye molecules, breaking them down into smaller and less harmful products like carbon dioxide ( $CO_2$ ) and water ( $H_2O$ ).

- Additional Considerations

Hydroperoxyl radicals ( $HO^\bullet$ ) can also participate in dye degradation by reacting with water molecules to generate hydrogen peroxide ( $H_2O_2$ ) and another hydroxyl radical ( $OH^\bullet$ ), as shown in Equation 10. Minimizing the recombination of photogenerated electrons and holes is crucial for efficient photocatalytic activity.



To summarize, the photocatalytic degradation of dyes by  $Cs_2Ag_xNa_{1-x}InCl_6$  involves light-induced charge separation, followed by a series of redox reactions with oxygen and water molecules. The generated reactive oxygen species, primarily hydroxyl radicals, are responsible for the breakdown of organic pollutants.

### 3.4.3 Factors affecting photocatalysis

In general terms the oxidation rates and productivity of the photocatalytic systems highly rely on various operational parameters that control the photo-degradation of organic molecules. A number of case studies have reported the significance of these operational parameters. The photo-degradation depends upon some of the basic parameters mentioned below:

- Concentration of substrate
- Amount of photocatalyst
- The pH of solution
- Temperature of reaction medium
- Time of irradiation of light
- The intensity of light
- Surface area of photocatalyst
- Dissolve oxygen in the reaction medium
- Nature of the photocatalyst
- Nature of the substrate
- Doping of metal ions and non-metal
- Structure of photocatalyst and substrate

Hence, the photo-degradation of organic compounds has been studied by a number of scientists and researchers; so a final conclusion is made that the optimum conditions for the photo-degradation of organic compounds must rely upon above parameters. With the passage of time new and different strategies have been applied. For example surface and interface modification by managing particle size and shape, composite or coupling materials, doping of transition metal, doping of nonmetal, application of co-doping (like; metal–metal, metal–nonmetal, nonmetal–nonmetal), deposition of noble metal, and by the use of organic dye and metal complexes sensitization of surface, in order to enhance and boost the photocatalytic properties.

## 4 Results and Discussion

### 4.1 X Ray Diffraction (XRD)

The PXRD data was collected on the prepared ground sample with  $2\theta$  varying from  $10^\circ$  to  $80^\circ$  with a step size of  $0.02^\circ$  using Copper  $K\alpha$  radiation of wavelength  $1.5408\text{\AA}$  on the Rigaku SmartLab X-Ray Diffractometer at ULMC of Goa University. The collected Data was subjected to refinement using FullProf software.

The profile matching refinements carried out on the PXRD data indicate that all prepared samples have a cubic structure belonging to the Fm-3m space group.

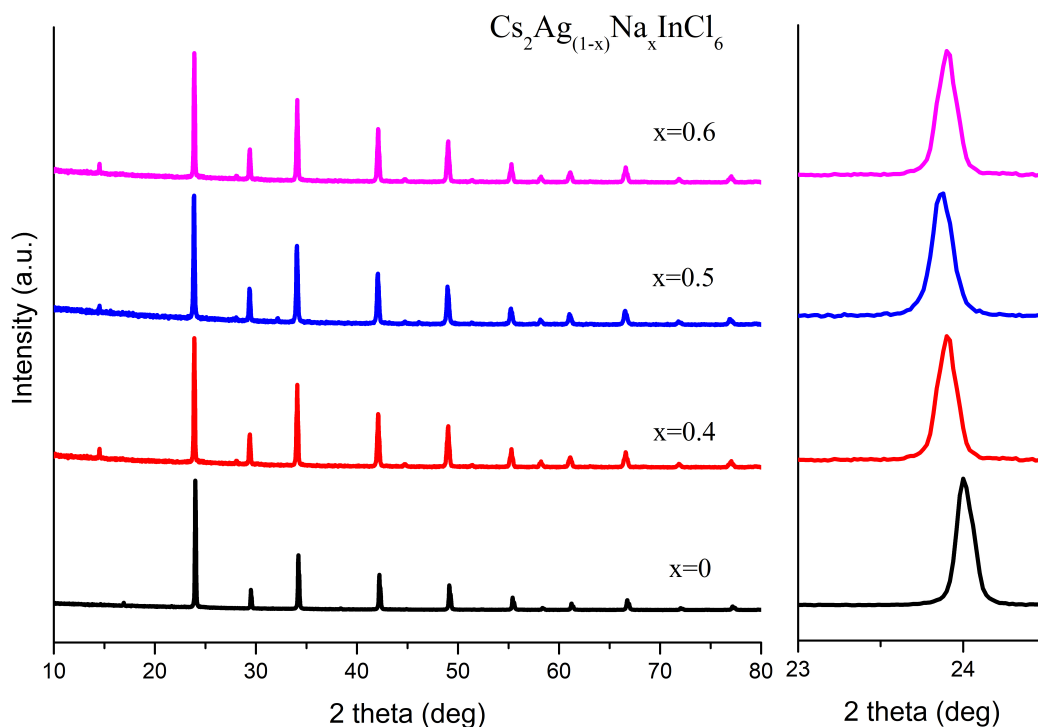


Figure 26: X ray Diffraction Patterns of synthesized  $Cs_2Ag_{(1-x)}Na_xInCl_6$

Fig.26 shows the comparison of XRD patterns. The sharp and intense Bragg peaks indicate that the samples have crystallized very well. The Bragg peaks shift towards lower  $2\theta$  values with increasing Na concentration indicating that the lattice parameter increases with the substitution of Na in the Ag sites.

The lattice parameters as given in table are seen to increase proportionally with increasing Na concentration further confirming Na doping.

Table 1: Compound, Lattice Parameter, and Direct Cell Volume

Compound	$Cs_2Ag_{(1-x)}Na_xInCl_6$	Lattice Parameter ( $\text{\AA}$ )	Unit Cell Volume ( $\text{\AA}^3$ )
$x = 0$		10.4772	1150.03
$x = 0.4$		10.5111	1161.48
$x = 0.5$		10.5160	1163.20
$x = 0.6$		10.5000	1157.75

The plots of profile matching for are shown below the series of  $Cs_2Ag_{(1-x)}Na_xInCl_6$ .

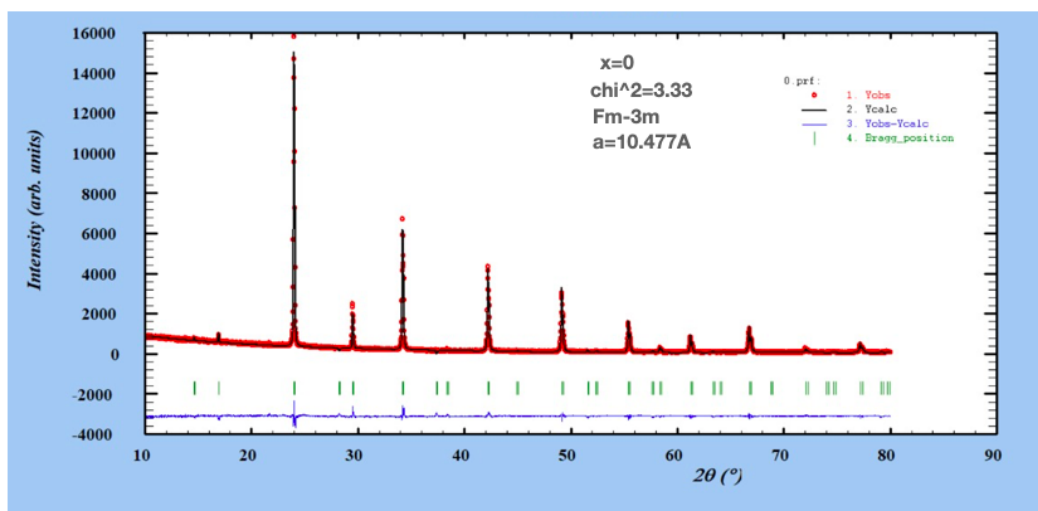


Figure 27: Profile matching for the series of  $Cs_2Ag_{(1-x)}Na_xInCl_6$ . Where  $x=0$

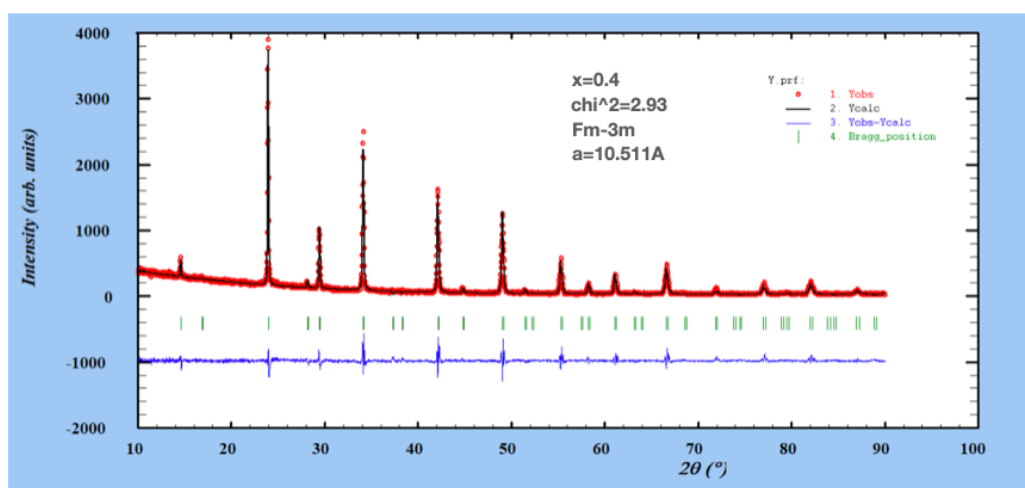


Figure 28: Profile matching for the series of  $Cs_2Ag_{(1-x)}Na_xInCl_6$ . Where  $x=0.4$

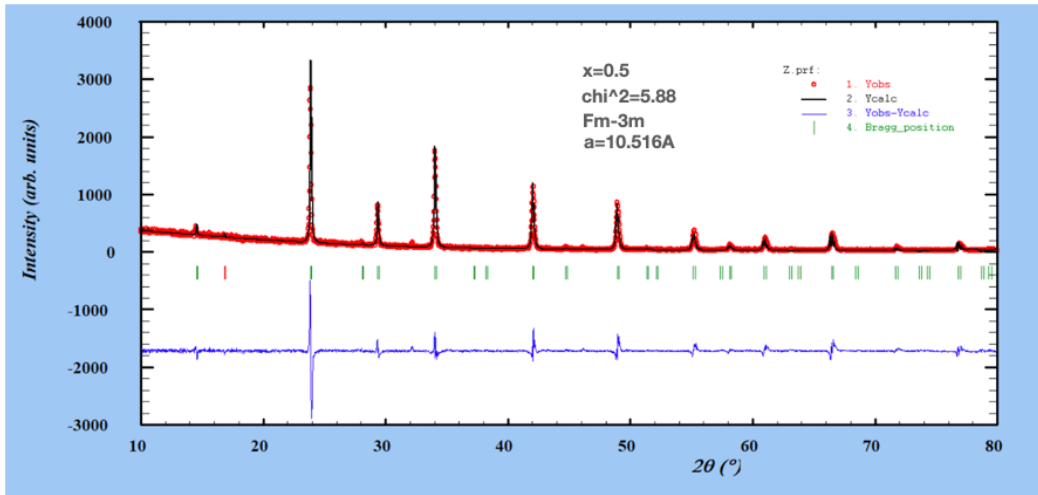


Figure 29: Profile matching for the series of  $Cs_2Ag_{(1-x)}Na_xInCl_6$ . Where  $x=0.5$

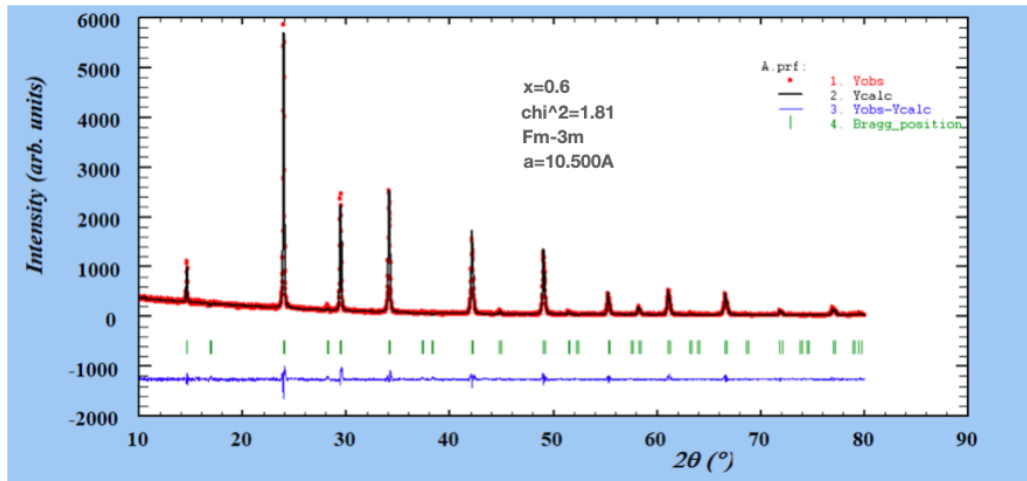


Figure 30: Profile matching for the series of  $Cs_2Ag_{(1-x)}Na_xInCl_6$ . Where  $x=0.6$

## 4.2 Scanning Electron Microscopy (SEM)

SEM images of the synthesized series  $Cs_2Ag_{(1-x)}Na_xInCl_6$  were taken using Zeiss Scanning Electron Microscope, we can see the particle formed with similar morphology and uniform size. The crystals were found to be in the range of around  $2\mu m$  to several tens of microns as can be seen from figures 31. The crystals are random in shape even though the unit cell is face centred cubic as confirmed by PXRD. It can be seen that the crystallites also show Agglomeration.

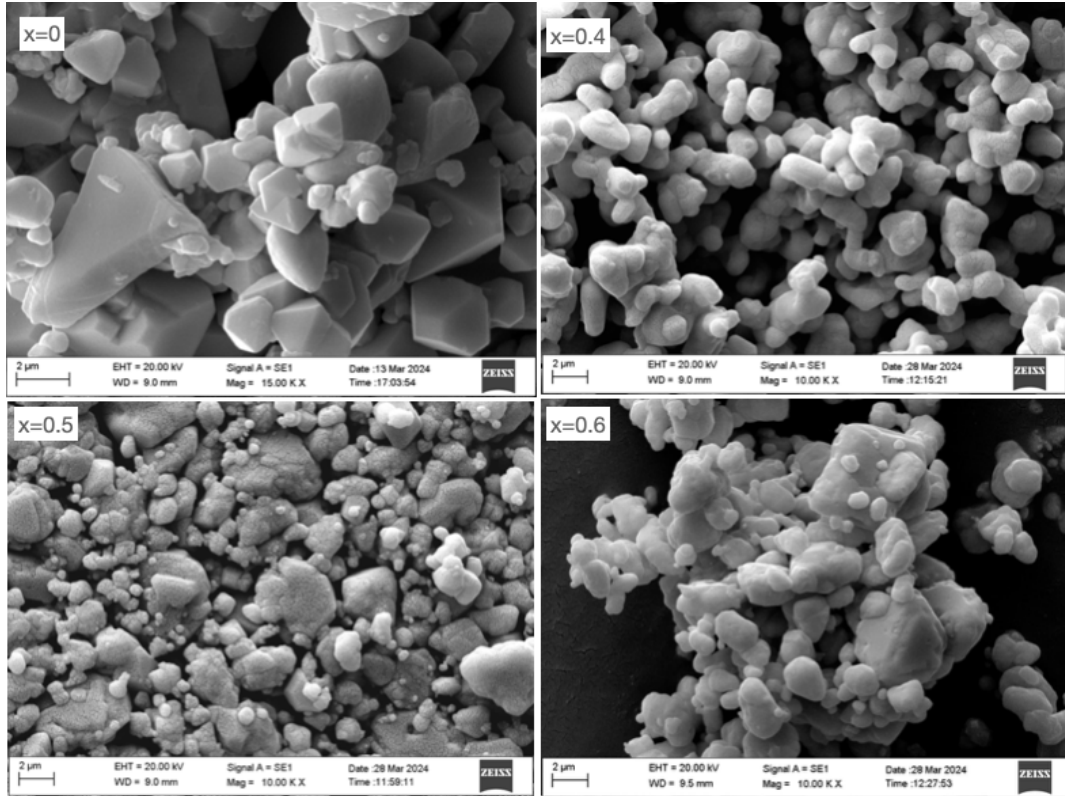


Figure 31: SEM image of series  $Cs_2Ag_{(1-x)}Na_xInCl_6$  with scale in all fig equal to  $2\mu m$ .

The random crystal structure is due to preferred stacking of the cubic unit cells.

### 4.3 Photocatalysis

One of the main objectives of this project was to test the prepared samples for photocatalytic applications. The dye of Methyl Orange ( $C_{14}H_{14}N_3NaO_3S$ ) for the photo-degradation experiments. The experiment was carried out in Lelesil UV-Vis Photochemical Reactor consisting of a 250W UV Lamp with a predominant wavelength of 280 nm. To prepare the dye stock solution, 5mg of Methyl Orange dye was dissolved in 50 ml of ethanol and stirred for half an hour. 5 ml of this stock solution was mixed with 45ml of ethanol to get the 10mg/L dye solution. 0.25mg of the compound was taken in 50 ml dye solution and stirred for one hour in the dark to reach adsorption-desorption equilibrium before turning on the UV Lamp. 3ml of this solution was taken out in a quartz cuvette using a syringe and absorbance spectra was recorded from 300nm to 600nm on Shimadzu UV-Vis Spectrophotometer. This step was repeated at ten minute intervals and the degradation of the dyes was observed.

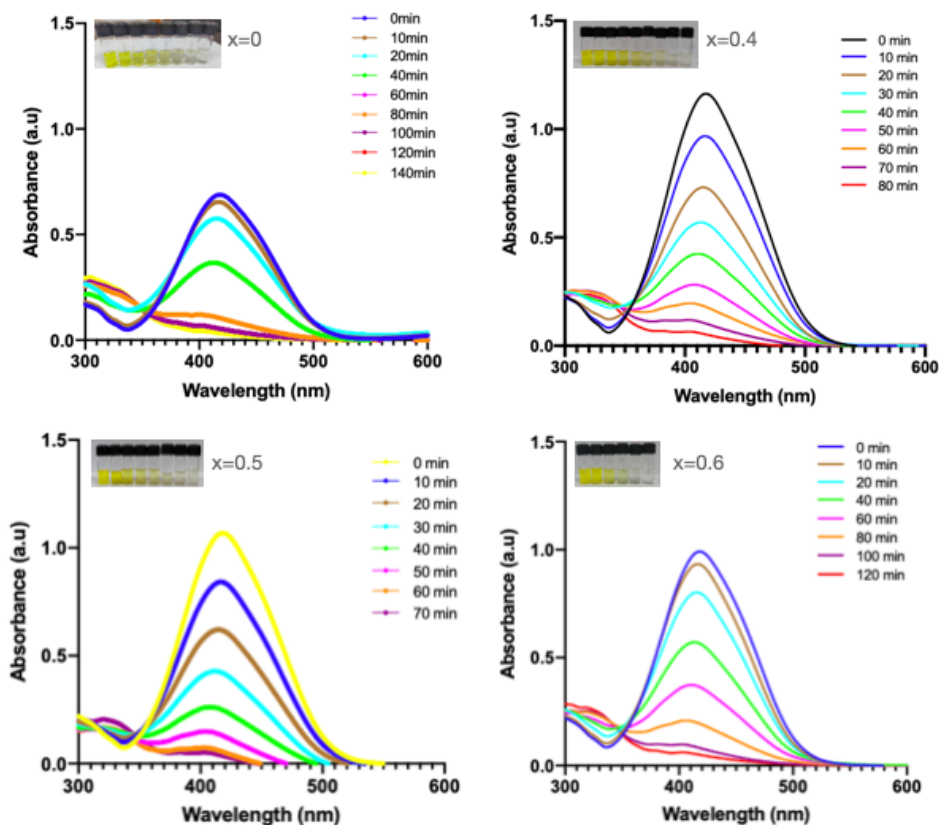


Figure 32: UV-Vis absorption spectra for Methyl Orange degradation in the presence of the series of  $Cs_2Ag_{(1-x)}Na_xInCl_6$  double perovskites under various UV-light irradiation times (The inset shows the change of solution colour)

Table 2: Compound and Time (min)

Compound $Cs_2Ag_{(1-x)}Na_xInCl_6$	Time (min)
$x = 0$	140
$x = 0.4$	80
$x = 0.5$	70
$x = 0.6$	120

Figure 31 shows the absorbance spectra of methyl orange solution degraded using the series of  $Cs_2Ag_{(1-x)}Na_xInCl_6$ .

From this, It has been observed that the characteristic absorption peak for methyl orange exists at 495 nm.

Using the absorption spectra data, plots  $C_t/C_0$  versus the irradiation time for photocatalytic degradation of Methyl Orange in the presence of  $Cs_2Ag_{(1-x)}Na_xInCl_6$  (figure 33) and Kinetic Curves of photocatalytic degradation reaction of Methyl Orange (figure 34) were obtained

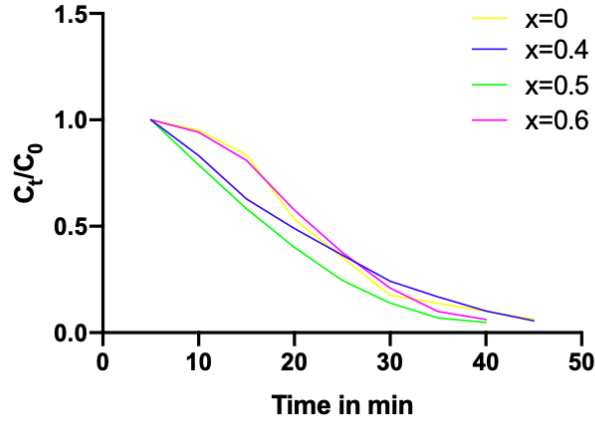


Figure 33: Plots of  $C_t/C_0$  versus the irradiation time for photocatalytic degradation of Methyl Orange in the presence of  $Cs_2Ag_{(1-x)}Na_xInCl_6$

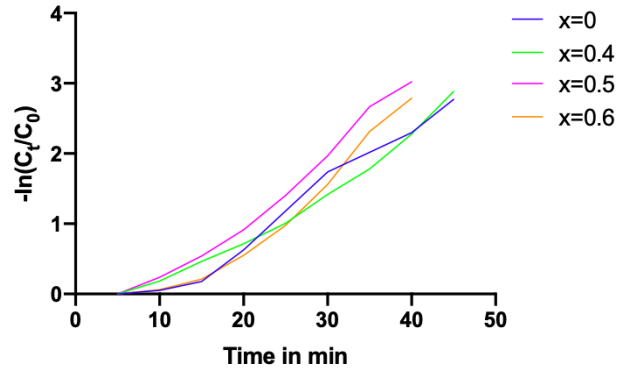


Figure 34: Kinetic Curves of photocatalytic degradation reaction of Methyl Orange

It is observed that the dye degrades fastest in the presence of  $Cs_2Ag_{0.5}Na_{0.5}InCl_6$  as the catalyst and the degradation rate decreases with increasing Na Concentration. This can be attributed to the fact that  $Cs_2AgInCl_6$  has a direct energy band gap and the incorporation Na induces an indirect band gap in the compounds as referenced in [64]

Table 3 gives the degradation rate constants of the dyes which are the slopes of the graphs in fig 34. These slopes have been calculated by fitting a linear curve through the graphs. Clearly the degradation is maximum and fastest in the presence of  $Cs_2AgInCl_6$  and decreases with increasing Na.

Table 3: Dye Degradation Constant (k value)

Compound $Cs_2Ag_{(1-x)}Na_xInCl_6$	Dye Degradation Constant (k value)
$x = 0$	0.10270
$x = 0.4$	0.07053
$x = 0.5$	0.09068
$x = 0.6$	0.08394

### 4.3.1 Comparison with other published works

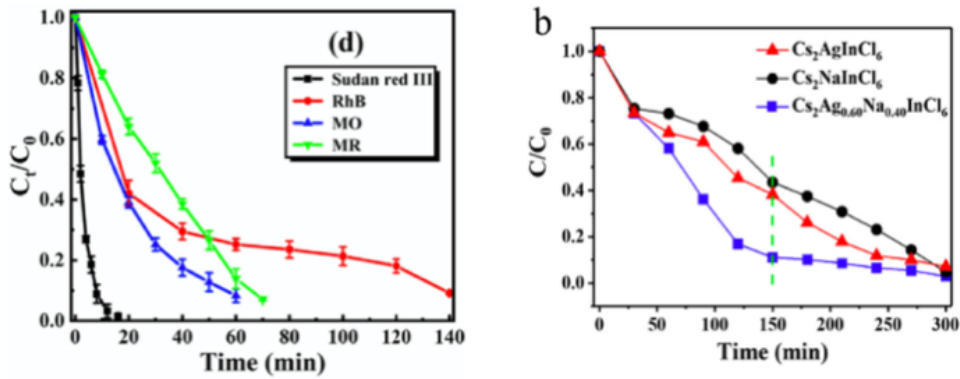


Figure 35: Degradation of organic dyes by (d)  $Cs_2AgInCl_6$  and (b)  $Cs_2Ag_{(1-x)}Na_xInCl_6$  [38] [64]

Many previous studies have reported the photocatalytic activity of undoped  $Cs_2AgInCl_6$  for the degradation of organic pollutants. For instance, [[38][64]]. The results of these studies can be used as a benchmark to evaluate the impact of Na doping on the photocatalytic performance of  $Cs_2AgInCl_6$ . In our study, all Na-doped  $Cs_2AgInCl_6$  perovskites exhibited higher photocatalytic activity for MO degradation compared to previous reports on undoped  $Cs_2AgInCl_6$ . This suggests that Na doping has a beneficial effect on the photocatalytic properties of  $Cs_2AgInCl_6$ , potentially by enhancing light absorption, promoting charge separation, or improving the surface reactivity of the material.

Our investigation identified  $Cs_2AgIn_{0.5}Na_{0.5}Cl_6$  ( $x = 0.5$ ) as the most efficient photocatalyst for MO degradation among the synthesized materials. This finding partially contrasts with the work of Sun et al.(2021) [64], who reported  $Cs_2AgIn_{0.4}Na_{0.6}Cl_6$  ( $x = 0.6$ ) to exhibit the optimal photocatalytic activity for the degradation of rhodamine B under visible light irradiation. This discrepancy in the optimal Na doping level ( $x = 0.5$  vs.  $x = 0.6$ ) for achieving maximum photocatalytic performance can be attributed to several factors.

One key difference between the two is the synthesis method employed. In this study, we used the acid precipitation method of synthesis which gave the product in powder form, while Sun et al. (2021)[64] employed hydrothermal synthesis to produce crystals which were then ground to powder. Synthesis methods can significantly influence the synthesised material's morphology, crystallinity, and defect structures, all of which can impact its photocatalytic activity. Another factor that can be considered is the potential variations in the specific UV light source characteristics (wavelength intensity, irradiation time) or other experimental details (initial MO concentration, catalyst dosage etc) between the two studies.

## 5 Conclusion

- Powdered crystalline samples of  $Cs_2Ag_{(1-x)}Na_xInCl_6$  were prepared using time efficient and simple acid precipitation method.
- The samples were subjected to refinement using Fullprof software and the lattice parameteres were verified from profile matching.
- The compounds crystallize in random shape as seen in SEM images with a face centred cubic unit cell belonging to the Fm-3m space.
- The samples exhibit good photocatalytic behavior and were able degrade Methyl orange efficiently in the presence of UV light.
- The sample with  $x=0.5$  exhibits the best photocatalytic property of all,able degrade dye in 70 mins
- The photocatalytic property is shown to decrease with increasing Na concentration.

## References

- [1] *Assay Guidance Manual*. Eli Lilly & Company and the National Center for Advancing Translational Sciences, Bethesda (MD), 2004.
- [2] Mohammad Adil Afroz, Anupriya Singh, Ritesh Kant Gupta, Rabindranath Garai, Naveen Kumar Tailor, Yukta, Shivani Choudhary, Bhavna Sharma, Prerna Mahajan, Bhavya Padha, Sonali Verma, Sandeep Arya, Vinay Gupta, Seckin Akin, Daniel Prochowicz, Mohammad Mahdi Tavakoli, S. P. Singh, Parameswar K. Iyer, Pankaj Yadav, Hanlin Hu, Goutam De, and Soumitra Satapathi. Design potential and future prospects of lead-free halide perovskites in photovoltaic devices. *J. Mater. Chem. A*, 11:13133–13173, 2023.
- [3] Robert Baan, Kurt Straif, Yann Grosse, Béatrice Secretan, Fatiha El Ghissassi, Véronique Bouvard, Lamia Benbrahim-Tallaa, and Vincent Coglianò. Carcinogenicity of some aromatic amines, organic dyes, and related exposures. *The Lancet Oncology*, 9(4):322–323, Apr 2008.
- [4] Amit Bafana, Sivanesan Saravana Devi, and Tapan Chakrabarti. Azo dyes: past, present and the future. *Environmental Reviews*, 19(NA):350–371, 2011.
- [5] Krzysztof Bienkowski, Renata Solarska, Linh Trinh, Justyna Widera-Kalinowska, Basheer Al-Anesi, Maning Liu, G. Krishnamurthy Grandhi, Paola Vivo, Burcu Oral, Beyza Yılmaz, and Ramazan Yıldırım. Halide perovskites for photoelectrochemical water splitting and co2 reduction: Challenges and opportunities. *ACS Catalysis*, pages 6603–6622, Apr 2024.
- [6] D. L. Bish, editor. *Modern Powder Diffraction*, volume 20 of *Reviews in Mineralogy*. Mineralogical Society of America, 1989.
- [7] J.A. Caram, M.J. Banera, J.F. Martínez Suárez, and M.V. Mirífico. Electrochemical behaviour of anthraquinone dyes in non aqueous solvent solution.: Part i. medium effect on the electrochemical behaviour. *Electrochimica Acta*, 249:431–445, 2017.
- [8] Liyan Chen, Hangjie Jiang, Zhaohua Luo, Guoqiang Liu, Xianhui Wu, Yongfu Liu, Peng Sun, and Jun Jiang. Enhancement of the efficiency and thermal stability of the double perovskite  $\text{Cs}_2\text{AgInCl}_6$  single crystal by  $\text{Sc}^{3+}$  substitution††electronic supplementary information (esi) available. see doi: <https://doi.org/10.1039/d2ma00139j>. *Materials Advances*, 3(10):4381–4386, 2022.
- [9] Vien Cheung. Colour: its influence and impact on the way we live. *Spotlight*, University of Leeds, 2018.
- [10] Kenneth Cole and Barry S. Levine. *Ultraviolet-Visible Spectrophotometry*, pages 127–134. Springer International Publishing, Cham, 2020.
- [11] Shimadzu Corporation. Uv-vis spectroscopy.
- [12] B. D. Cullity. *Elements of X-ray diffraction*. Addison-Wesley, 1978.
- [13] Andrey G. Kostianoy Damià Barceló. *The Handbook of Environmental Chemistry*. Springer, 1982.
- [14] Brian L. Diffey. Sources and measurement of ultraviolet radiation. *Methods*, 28(1):4–13, 2002.
- [15] J. W. Drexler and T. E. Everhart. High-resolution scanning electron microscopy. *Physical Review B*, 2(12):2584, 1970.
- [16] G.Nelson Eby. *Principles of environmental geochemistry*. Thomson-Brooks/Cole, Australi, 2004.
- [17] European Food Safety Authority (EFSA). Assessment of the results of the study by mccann et al. (2007) on the effect of some colours and sodium benzoate on children’s behaviour - scientific opinion of the panel on food additives, flavourings, processing aids and food contact materials (afc). *EFSA Journal*, 6(3):660, 2008.
- [18] Inc. Encyclopædia Britannica. Scanning electron microscope.
- [19] Diógenes Frederichi, Mara Scaliante, and Rosangela Bergamasco. Structured photocatalytic systems: photocatalytic coatings on low-cost structures for treatment of water contaminated with micropollutants—a short review. *Environmental Science and Pollution Research*, 28, 05 2021.
- [20] V. M. Goldschmidt. Crystal structure and chemical constitution. *Trans. Faraday Soc.*, 25:253–283, 1929.

- [21] J. Goldstein, D. E. Newbury, P. Echlin, D. C. Joy, C. E. Lyman, E. Lifshin, ..., and L. Colby. *Scanning electron microscopy and X-ray microanalysis*, volume 3. Springer Nature, 2017.
- [22] Kai Guo, Pei Lin, Di Wu, Zhifeng Shi, Xu Chen, Yanbing Han, Yongtao Tian, and Xinjian Li. Cs<sub>2</sub>AgBiCl<sub>6</sub>: a novel, High-Efficient and stable Visible-Light photocatalyst for degradation of organic dyes. *Chemistry*, 29(35):e202300400, May 2023.
- [23] Robert M. Hazen. Perovskites. *Scientific American*, 258(6):74–81, 1988.
- [24] M. R. Hoffmann, A. J. Hoffmann, and H. Herrmann. *Environmental Applications of Semiconductor Photocatalysis*. CRC Press, 1995.
- [25] Aslam Hossain, Prasanta Bandyopadhyay, and Sanjay Roy. An overview of double perovskites a<sub>2</sub>bbo<sub>6</sub> with small ions at a site: Synthesis, structure and magnetic properties. *Journal of Alloys and Compounds*, 740:414–427, 12 2017.
- [26] Muhammad Ikram, Muhammad Ahsaan Bari, and Junaid Haider. *Photocatalytic Dye Degradation Using Green Polymer-Based Nanostructures*. 2053-2563. IOP Publishing, 2023.
- [27] LLC Innovatech Labs. The advantages and disadvantages of scanning electron microscopy (sem). Web-page, 2020.
- [28] Muhammad Ismail, Kalsoom Akhtar, M I Khan, Tahseen Kamal, Murad A Khan, Abdullah M Asiri, Jongchul Seo, and Sher B Khan. Pollution, toxicity and carcinogenicity of organic dyes and their catalytic Bio-Remediation. *Curr Pharm Des*, 25(34):3645–3663, 2019.
- [29] Jun Jiang, Yao Li, Xiaolong Liu, Shun Luo, and Lixia Sun. Phthalocyanine-based materials for photocatalytic hydrogen evolution. *Advanced Materials*, 29(14):1700703, 2017.
- [30] Pankaj P. Khirade and Anil V. Raut. Perovskite structured materials: Synthesis, structure, physical properties and applications. In Poorva Sharma and Ashwini Kumar, editors, *Recent Advances in Multifunctional Perovskite Materials*, chapter 1. IntechOpen, Rijeka, 2022.
- [31] Jennifer Kirby and Richard White. The fading of some nitro dyes: a combined chromatographic and mass spectrometric study. *Studies in Conservation*, 45(2):87–95, 2000.
- [32] Gaurav Kumar. Kumar 2019 j. phys. conf. ser. 1240 012161. 10 2020.
- [33] Manish Kumar, Manjari Jain, Arunima Singh, and Saswata Bhattacharya. Sublattice mixing in Cs<sub>2</sub>AgInCl<sub>6</sub> for enhanced optical properties from first-principles. *Applied Physics Letters*, 118(2):021901, 01 2021.
- [34] Po-Kai Kung, Ming-Hsien Li, Pei-Ying Lin, Jia-Yun Jhang, Martina Pantaler, Doru C. Lupascu, Giulia Grancini, and Peter Chen. Lead-free double perovskites for perovskite solar cells. *Solar RRL*, 4(2):1900306, 2020.
- [35] Joseph Lakowicz. *Principles of Fluorescence Spectroscopy*, volume 1. 01 2006.
- [36] K. Lenz, M. Bauer, S. Deutsch, P. Duda, C. Fimpel, M. Jaeger, N. Kaefer, C. Kail, C. Kolbeck, G. Lambertz, et al. Photocatalysis: Introduction, mechanism, and effective parameters. *ChemEngineering*, 4(4):48, 2020.
- [37] Junming Li, Hai-Lei Cao, Wen-Bin Jiao, Qiong Wang, Mingdeng Wei, Irene Cantone, Jian Lü, and Antonio Abate. Biological impact of lead from halide perovskites reveals the risk of introducing a safe threshold. *Nature Communications*, 11(1):310, Jan 2020.
- [38] Keke Li, Sen Li, Wule Zhang, Zhifeng Shi, Di Wu, Xu Chen, Pei Lin, Yongtao Tian, and Xinjian Li. Highly-efficient and stable photocatalytic activity of lead-free cs<sub>2</sub>agincl<sub>6</sub> double perovskite for organic pollutant degradation. *Journal of Colloid and Interface Science*, 596:376–383, 2021.
- [39] Jiajun Luo, Shunran Li, Haodi Wu, Ying Zhou, Yang Li, Jing Liu, Jinghui Li, Kanghua Li, Fei Yi, Guangda Niu, and Jiang Tang. Cs<sub>2</sub>agincl<sub>6</sub> double perovskite single crystals: Parity forbidden transitions and their application for sensitive and fast uv photodetectors. *ACS Photonics*, 5, 10 2017.

- [40] Iago López-Fernández, Donato Valli, Chun-Yun Wang, Subarna Samanta, Takuya Okamoto, Yi-Teng Huang, Kun Sun, Yang Liu, Vladimir S. Chirvony, Avijit Patra, Juliette Zito, Luca De Trizio, Deepika Gaur, Hong-Tao Sun, Zhiguo Xia, Xiaoming Li, Haibo Zeng, Iván Mora-Seró, Narayan Pradhan, Juan P. Martínez-Pastor, Peter Müller-Buschbaum, Vasudevanpillai Biju, Tushar Debnath, Michael Saliba, Elke Debroye, Robert L. Z. Hoyer, Ivan Infante, Liberato Manna, and Lakshminarayana Polavarapu. Lead-free halide perovskite materials and optoelectronic devices: Progress and perspective. *Advanced Functional Materials*, 34(6):2307896, 2024.
- [41] Rishabha Malviya, Vvipin Bansal, Om Pal, and Pramod Sharma. High performance liquid chromatography: A short review. *Journal of Global Pharma Technology*, 2:22–26, 06 2010.
- [42] Sukanya Mehra, Mandeep Singh, and Pooja Chadha. Adverse impact of textile dyes on the aquatic environment as well as on human beings. *Toxicology International*, 28(2):165–176, May 2021.
- [43] Edson Meyer, Dorcas Mutukwa, Nyengerai Zingwe, and Raymond Taziwa. Lead-free halide double perovskites: A review of the structural, optical, and stability properties as well as their viability to replace lead halide perovskites. *Metals*, 8(9), 2018.
- [44] Yuncheng Mu, Ziyu He, Kun Wang, Xiaodong Pi, and Shu Zhou. Recent progress and future prospects on halide perovskite nanocrystals for optoelectronics and beyond. *iScience*, 25(11):105371, October 2022.
- [45] Ankan Mukhopadhyay. Measurement of magnetic hysteresis loops in continuous and patterned ferromagnetic nanostructures by static magneto-optical kerr effect magnetometer. 07 2015.
- [46] Paco Noriega and Edison Osorio. *Mass Spectrometry and Its Importance for the Analysis and Discovery of Active Molecules in Natural Products*. 05 2021.
- [47] David O. Obada, Shittu B. Akinpelu, Simeon A. Abolade, Emmanuel Okafor, Aniekan M. Ukpong, Syam Kumar R, and Akinlolu Akande. Lead-free double perovskites: A review of the structural, optoelectronic, mechanical, and thermoelectric properties derived from first-principles calculations, and materials design applicable for pedagogical purposes. *Crystals*, 14(1), 2024.
- [48] Qingdong Ou, Xiaozhi Bao, Yinan Zhang, Huaiyu Shao, Guichuan Xing, Xiangping Li, Liyang Shao, and Qiaoliang Bao. Band structure engineering in metal halide perovskite nanostructures for optoelectronic applications. *Nano Materials Science*, 1(4):268–287, 2019. Special Issue on two-dimensional nanomaterials.
- [49] Malvern Panalytical. Solutions.
- [50] Malvern Panalytical. X-ray diffraction (xrd) - overview.
- [51] D. L. Pavia. *Introduction to spectroscopy*. Brooks/Cole, 3 edition, 2001.
- [52] Aravin Prince Periyasamy. Recent advances in the remediation of textile-dye-containing wastewater: Prioritizing human health and sustainable wastewater treatment. *Sustainability*, 16(2), 2024.
- [53] L. Reimer, editor. *Scanning electron microscopy*, volume 49. Springer Science Business Media, 1998.
- [54] Rigaku. Smartlab se — rigaku global website. Webpage.
- [55] Bryan A. Rosales, Michael P. Hanrahan, Brett W. Boote, Aaron J. Rossini, Emily A. Smith, and Javier Vela. Lead halide perovskites: Challenges and opportunities in advanced synthesis and spectroscopy. *ACS Energy Letters*, 2(4):906–914, Apr 2017.
- [56] Thermo Fisher Scientific. Energy-dispersive x-ray spectroscopy (eds) analysis with sem.
- [57] Thermo Fisher Scientific. Uv-vis spectrophotometry.
- [58] SciMed. Scanning electron microscopy (sem). Webpage.
- [59] SERC. X-ray powder diffraction (xrd).
- [60] Robert Shannon. Revised effective ionic radii and systematic studies of interatomic distances in halides and chalcogenides. *Acta Cryst*, 32:751–767, 01 1976.

- [61] Manoj Sharma, Tarun Jain, Sukhvir Singh, and O.P. Pandey. Photocatalytic degradation of organic dyes under uv–visible light using capped zns nanoparticles. *Solar Energy*, 86(1):626–633, 2012.
- [62] Aarti Singh, Anupama Mittal, and Nirmala Jangid. *Toxicology of Dyes*, pages 50–69. 01 2020.
- [63] Sonika Singh, Gurjiwan Sidhu, and Harminder Singh. Removal of methylene blue dye using activated carbon prepared from biowaste precursor. *Indian Chemical Engineer*, pages 1–12, 12 2017.
- [64] Jifu Sun, Zhijuan Yang, Longzhi Li, Yue Zhang, and Guifu Zou. Highly stable halide perovskite with na incorporation for efficient photocatalytic degradation of organic dyes in water solution. *Environmental Science and Pollution Research*, 28(22):50813–50824, 2021.
- [65] Marcela G. R. Tavares, Danilo H. S. Santos, Mariana G. Tavares, José L. S. Duarte, Lucas Meili, Wagner R. O. Pimentel, Josealdo Tonholo, and Carmem L. P. S. Zanta. Removal of reactive dyes from aqueous solution by fenton reaction: Kinetic study and phytotoxicity tests. *Water, Air, & Soil Pollution*, 231(2):82, Feb 2020.
- [66] Md Uddin, Arif Hasan, Sharif-Ar Raffi, and Sabrina Afrin. Uddin et al 2015 - protoplast fusion and culture, 06 2015.
- [67] Motohiro Uo, Takahiro Wada, and Tomoko Sugiyama. Applications of x-ray fluorescence analysis (xrf) to dental and medical specimens. *Japanese Dental Science Review*, 01 2014.
- [68] Aili Wang, Chuantian Zuo, Xiaobin Niu, Liming Ding, Jianning Ding, and Feng Hao. Recent promise of lead-free halide perovskites in optoelectronic applications. *Chemical Engineering Journal*, 451:138926, 2023.
- [69] J. Workman, Jr. *Applied spectroscopy*. Elsevier, 2011.
- [70] M. Yashima and Y. Hashimoto. X-ray diffraction (xrd) technique for material characterization. *Journal of Chemical Education*, 74(8):808, 1997.
- [71] Zhiguo Zhang, Yuping Liu, Qiang Sun, Huaxia Ban, Zhirong Liu, Huaixuan Yu, Xiongjie Li, Letian Dai, Wanpeng Yang, Yan Shen, and Mingkui Wang. The importance of elemental lead to perovskites photo-voltaics. *Chemistry of Inorganic Materials*, 1:100017, 2023.
- [72] Ting Zhong, Haibo Zhu, Yeye Zheng, Gaowen Ren, Xinmei Xie, Qiangwen Fan, Zong-Bo Xie, and Zhang-Gao Le. Lead-free cs<sub>2</sub>agbibr<sub>6</sub> double perovskite microcrystals for effective visible-light photocatalytic thio/selenocyanation. *Chemical Communications*, 60, 03 2024.
- [73] (Analytical Techniques Group) . Ultraviolet–visible spectroscopy. *Chemical Society Reviews*, 21(1):73–88, 1992.